frontiers in Astronomy and Space Sciences

ORIGINAL RESEARCH
published: 29 March 2021
doi: 10.3389/fspas.2021.624907

Check for updates

# Search for (sub)stellar Companions of Exoplanet Hosts by Exploring the Second ESA-Gaia Data Release

*K.-U. Michel* and M. Mugrauer*

*Astrophysikalisches Institut und Universitäts-Sternwarte Jena, Jena, Germany*

We present the latest results of an ongoing multiplicity survey of exoplanet hosts, which was initiated at the Astrophysical Institute and University Observatory Jena, using data from the second data release of the ESA-Gaia mission. In this study the multiplicity of 289 targets was investigated, all located within a distance of about 500 pc from the Sun. In total, 41 binary, and five hierarchical triple star systems with exoplanets were detected in the course of this project, yielding a multiplicity rate of the exoplanet hosts of about 16%. A total of 61 companions (47 stars, a white dwarf, and 13 brown dwarfs) were detected around the targets, whose equidistance and common proper motion with the exoplanet hosts were proven with their precise Gaia DR2 astrometry, which also agrees with the gravitational stability of most of these systems. The detected companions exhibit masses from about 0.016 up to 1.66 $M_{\odot}$ and projected separations in the range between about 52 and 9,555 au.

**Keywords: Multiple stars, white dwarfs, brown dwarfs, exoplanets, ESA-Gaia DR2**

OPEN ACCESS

***Edited by:***
*Rachel Matson,*
*United States Naval Observatory (USNO), United States*

***Reviewed by:***
*Claudio Melo,*
*European Southern Observatory, Chile*
*Robert De Rosa,*
*European Southern Observatory, Chile*

****Correspondence:***
*K.-U. Michel*
*kai-uwe.michel@uni-jena.de*

***Specialty section:***
*This article was submitted to Exoplanets, a section of the journal Frontiers in Astronomy and Space Sciences*

***Received:*** *01 November 2020*
***Accepted:*** *25 January 2021*
***Published:*** *29 March 2021*

***Citation:***
*Michel K-U and Mugrauer M (2021) Search for (sub)stellar Companions of Exoplanet Hosts by Exploring the Second ESA-Gaia Data Release. Front. Astron. Space Sci. 8:624907. doi: 10.3389/fspas.2021.624907*

## 1 INTRODUCTION

Since the detection of the first planet orbiting a star other than the Sun, several thousands of these exoplanets have been discovered by various detection techniques. While the majority of stars are members of multiple star systems (Duchêne and Kraus, 2013), most of the exoplanet host stars are single stars. Nevertheless several multiple star systems hosting exoplanets, could already be revealed by previous multiplicity studies using seeing limited or high contrast AO imaging observations (see e.g. Mugrauer et al., 2014; Mugrauer and Ginski, 2015). In order to explore the effects of the presence of stellar companions on the formation process and orbital evolution of exoplanets, a survey was initiated at the Astrophysical Institute and University Observatory Jena (described in detail by Mugrauer, 2019) to identify and characterize companions of exoplanet host stars, detected in the second data release of the European Space Agency (ESA) Gaia mission (Gaia DR2 from hereon, Gaia Collaboration et al., 2018). Furthermore, in Mugrauer and Michel (2020) a comparable investigation was carried out among potential exoplanet host stars, identified by the TESS mission (Ricker et al., 2015). The study, whose results are presented here, is the third work in the context with Mugrauer (2019). The following section gives a detailed description of this study, and the detected companions and their derived properties are presented in the third section of this paper.

## 2 GAIA DR2 SEARCH FOR (SUB)STELLAR COMPANIONS OF EXOPLANET HOSTS

The Gaia DR2 is based on data taken by the Gaia spacecraft in the first 22 months of its mission and contains 1.7 billion detected sources up to a limiting magnitude of $G = 21$ mag. For 1.3 billion sources a five parameter astrometric solution could be derived, i.e. beside their equatorial coordinates (α, δ), also the parallax $\pi$ and proper motion ($\mu_\alpha \cos(\delta)$, $\mu_\delta$) of these sources were determined. Furthermore, for about 88 million detected objects estimates of their G-band extinction and effective temperature are listed in the Gaia DR2, determined by the Priam algorithm, which is part of the astrophysical parameters inference system (Apsis, see Bailer-Jones et al., 2013) in the Gaia data processing.

Using Gaia DR2 data Mugrauer (2019) already explored the multiplicity of all exoplanet host stars, whose exoplanets were detected either by photometric transit observations, radial-velocity (RV), or astrometric measurements, and were listed in the Extrasolar Planets Encyclopedia[1] (EPE from hereon, Schneider et al., 2011) by mid of October 2018. The study, presented in this paper, complements this survey by investigating the multiplicity of the exoplanet hosts (stars but also brown dwarfs), whose planets were indirectly detected either via RV measurements or transit observations in the range of time between mid of October 2018 until end of September 2020, as well as all exoplanet hosts, known so far, with planets, which were directly detected by imaging observations. At the end of September 2020 the EPE lists about 4,350 exoplanets, and about 400 of them were detected around the hosts studied in this work.

(Sub)stellar Companions are expected to be located at the same distance to the Sun as the exoplanet hosts and form common proper motion pairs with them, in particular wide companions with projected separations of hundreds and thousands of au, i.e. the typical targets of this study. Hence, in order to clearly detect such companions and to prove the equidistance of these objects and the exoplanet hosts, in this study we have taken into account only Gaia DR2 sources with an accurate five parameter astrometric solution, i.e. which exhibit precise measurements of their parallax ($\pi/\sigma(\pi) > 3$) and proper motion ($\mu/\sigma(\mu) > 3$). Thereby, sources with negative parallaxes are neglected. As in the Gaia DR2 a parallax uncertainty of 0.7 mas is reached for faint sources down to $G = 20$ mag, the survey is furthermore constrained to exoplanet hosts, which are located within a distance of 500 pc around the Sun (i.e. $\pi > 2$ mas), to assure $\pi/\sigma(\pi) > 3$ even for the faintest companions, detectable in this survey. This distance constraint is slightly relaxed to $\pi + 3\sigma(\pi) \gtrapprox 2$ mas, i.e. taking into account also the parallax uncertainty of the hosts. By the end of September 2020, in total 289 exoplanet hosts are listed in the EPE, which fulfill this distance constraint, and hence are selected as targets for this study. The properties of all targets are summarized in **Table 1** and their histograms are illustrated in **Figure 1**. On average, the targets are solar like stars most frequently found within 150 pc around the Sun, which exhibit proper motions in the range between about 2 and 10,400 mas/yr, and G-band magnitudes from about 3.7 to 20.8 mag. In particular, the sub-sample of direct imaging exoplanet hosts emerges as a peak in the age distribution at young ages, as all these targets are typically younger than 0.1 Gyr, in contrast to hosts of RV and transiting exoplanets, which are older than 1 Gyr in general.

**TABLE 1 |** The properties of all targets of this study. The corresponding histograms are shown in **Figure 1**.

| | Distance (pc) | μ (mas/yr) | G (mag) | Age (Gyr) | Mass ($M_\odot$) |
|---|---|---|---|---|---|
| Min | 1.8 | 1.7 | 3.7 | 0.001 | 0.016 |
| Max | 586 | 10,394 | 20.8 | 14.9 | 20 |
| Ave | 137 | 270 | 10.8 | 3.5 | 1.1 |
| Med | 94 | 65 | 10.7 | 2.1 | 1.0 |

The companion search radius, applied in this project around the selected targets, is limited to a maximal projected separation of 10,000 au, which guarantees that the majority of wide companions of the exoplanet hosts are detectable in this study, as described by Mugrauer (2019). This upper separation limit results in an angular search radius around the targets of $r[arc\sec] = 10\pi[\mathrm{mas}]$. Within this radius around the targets the companionship of all sources, listed in the Gaia DR2 with an accurate five parameter astrometric solution was investigated. For the verification of the equidistance of all detected sources with the associated exoplanet hosts, the difference $\Delta\pi$ between their parallaxes was calculated, taking into account also the excess noise of their astrometric solutions. Common proper motion of the detected sources and the targets was checked with the precise Gaia DR2 proper motions of the exoplanet hosts $\mu_{\mathrm{PH}}$ and the sources $\mu_{\mathrm{Comp}}$. In addition, we have also derived for all sources the differential proper motion: $\mu_{\mathrm{rel}} = |\mu_{\mathrm{PH}} - \mu_{\mathrm{comp}}|$, which yields the common proper motion index ($\mathrm{cpm-index} = |\mu_{\mathrm{PH}} + \mu_{\mathrm{comp}}|/\mu_{\mathrm{rel}}$), which characterizes the degree of common proper motion of the detected sources and the exoplanet hosts.

Following the companion identification procedure ($sig\text{-}\Delta\pi \leq 3$ and $\mathrm{cpm-index} \geq 3$), as defined by Mugrauer (2019) the majority of all sources ( > 99.88%), detected within the applied search radius around the targets, can clearly be excluded as companions, as they are either not located at the same distances as the exoplanet hosts and/or do not share a common proper motion with them. In contrast, for 61 detected objects their companionship with the targets could clearly be proven with their precise Gaia DR2 astrometry. For all these companions we have determined their relative astrometry to the exoplanet hosts (angular separation ρ, and position angle PA), as well as their projected separation *sep*, derived with their angular separation and the parallax of the targets.

The absolute G-band magnitude of all companions was derived from their apparent G-band photometry, the parallax of the associated exoplanet hosts, as well as their Apsis-Priam G-band extinction estimate, all listed in the Gaia DR2. If there was no extinction estimate given for a companion, the extinction estimate of the exoplanet host was used instead or if not available, its extinction estimate, listed in the StarHorse catalog (Anders et al., 2019). In the case that no G-band extinction is available at all it was derived from V-band extinction measurements of the exoplanet hosts, listed either in the VizieR data base[2] (Ochsenbein et al.,

[1]Online available at: http://exoplanet.eu/

[2]Online available at: https://vizier.u-strasbg.fr/

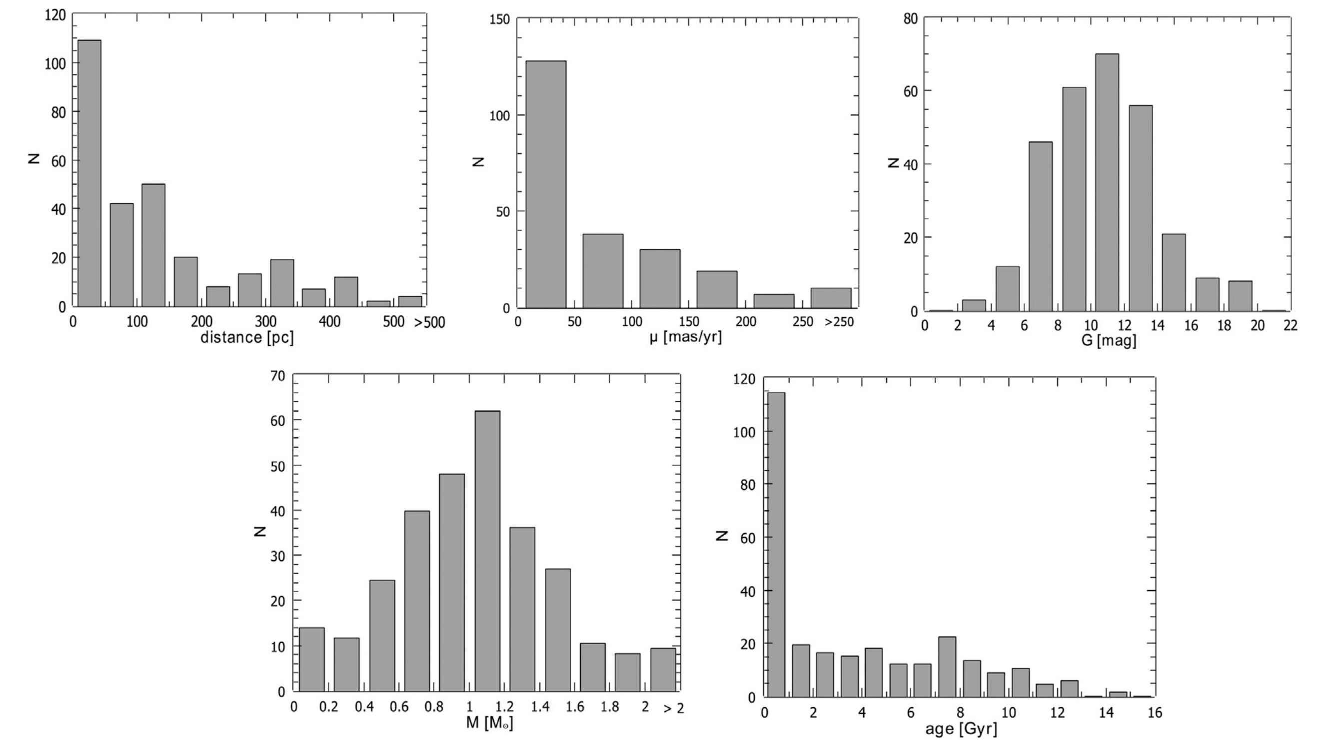


**FIGURE 1 |** The histograms of the individual properties of all targets of this study.

2000) or in the literature, adopting $A_G/A_V = 0.77$, as described by Mugrauer (2019).

The masses and effective temperatures of all detected companions were determined from their derived absolute G-band magnitudes using the evolutionary models of (sub)stellar objects from Baraffe et al. (2015), as well as the ages of the exoplanet hosts, as listed in the EPE. Thereby, we adopt the same age for the planet hosts and their companions. We determined the masses and effective temperatures of the companions via interpolation of the model grid with the age closest to that of the exoplanet hosts. For verification of the obtained results the properties of the companions derived from their G-band magnitudes were compared with those, determined from the near-infrared photometry, taken from the 2MASS Point Source catalog (Skrutskie et al., 2006), if available. For the near-infrared extinction we have used the relations: $A_{Ks}/A_V = 0.12$, $A_H/A_V = 0.17$, and $A_J/A_V = 0.26$, as described in Mugrauer (2019). A graphical comparison of the masses obtained from the G-band and the 2MASS photometry are shown in **Figure 2**. The identity is illustrated as gray dashed line in this figure. For all companions the derived masses agree well with each other, with deviations that remain below the $3\sigma$ level (the same holds also for the temperature estimates not shown here). Objects, whose masses were determined by extrapolation from the used model grids as such as those with bad quality (quality flags all but A) or contaminated 2MASS photometry were excluded in this comparison.

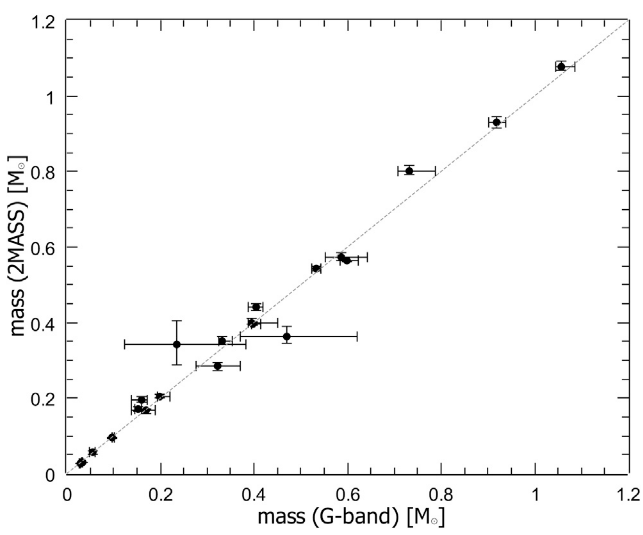


**FIGURE 2 |** Comparison of the mass of the detected companions, derived from their G-band and infrared 2MASS photometry.

Eventually for all companions, which were detected in this study, we have estimated their escape velocity $\mu_{esc}\,[\mathrm{mas\,yr^{-1}}] = 2\pi\sqrt{2M\pi_{PH}^3/\rho}$ with their angular separation ρ and the parallax of the associated exoplanet hosts both in the unit of milli-arcsec (mas), as well as the total mass $M$ of the system (in the unit $M_\odot$),

**TABLE 2 |** Gaia astro- and photometry of all exoplanet hosts and their companions, detected in this study.

| Name | $\pi$ (mas) | $\mu_\alpha \cos(\delta)$ (mas/yr) | $\mu_\delta$ (mas/yr) | epsi (mas) | sig-epsi | G (mag) | $A_G$ (mag) | |
|---|---|---|---|---|---|---|---|---|
| HD 1160 A* | 7.9417 ± 0.0764 | 20.089 ± 0.138 | −14.575 ± 0.099 | 0.121 | 6.0 | 7.1074 ± 0.0003 | $0.1347^{+0.1300}_{-0.0968}$ | |
| HD 1160 C | 6.9946 ± 0.2739 | 20.605 ± 0.333 | −16.215 ± 0.311 | 0.739 | 37 | 15.3505 ± 0.0207 | | |
| Gliese 49 A* | 101.4650 ± 0.0335 | 731.135 ± 0.041 | 90.690 ± 0.048 | — | — | 8.6628 ± 0.0007 | $0.6030^{+0.2220}_{-0.4095}$ | |
| Gliese 49 B | 101.6371 ± 0.0806 | 730.740 ± 0.163 | 86.352 ± 0.225 | 0.190 | 13 | 11.9238 ± 0.0033 | | |
| HD 8326 A* | 32.5591 ± 0.0466 | −58.470 ± 0.120 | −224.887 ± 0.064 | — | — | 8.4749 ± 0.0004 | | |
| HD 8326 B | 32.4362 ± 0.0589 | −57.577 ± 0.156 | −224.122 ± 0.088 | 0.347 | 27 | 14.2066 ± 0.0006 | $0.2940^{+0.2446}_{-0.0438}$ | |
| HD 13167 A* | 6.6859 ± 0.0485 | 43.770 ± 0.077 | −38.126 ± 0.079 | — | — | 8.1600 ± 0.0003 | | |
| HD 13167 B | 6.7931 ± 0.1254 | 44.134 ± 0.215 | −39.358 ± 0.212 | 0.444 | 3.3 | 17.4513 ± 0.0022 | $0.2431^{+0.0597}_{-0.0648}$ | SHC |
| HR 858 A* | 31.2565 ± 0.0700 | 123.229 ± 0.070 | 105.788 ± 0.151 | 0.086 | 3.9 | 6.2480 ± 0.0003 | $0.1320^{+0.1061}_{-0.0911}$ | |
| HR 858 B | 32.3014 ± 0.1670 | 137.125 ± 0.213 | 105.865 ± 0.302 | 0.835 | 63 | 16.0464 ± 0.0031 | | |
| HD 18015 A* | 8.0490 ± 0.0517 | 63.053 ± 0.089 | − 4.359 ± 0.082 | — | — | 7.7219 ± 0.0005 | | |
| HD 18015 B | 7.9413 ± 0.0415 | 64.638 ± 0.071 | − 4.668 ± 0.066 | — | — | 12.2361 ± 0.0008 | $0.1440^{+0.0361}_{-0.0325}$ | |
| K2-288 B* | 15.2166 ± 0.2007 | 185.476 ± 0.708 | −74.070 ± 0.618 | 0.766 | 70 | 14.5451 ± 0.0017 | | |
| K2-288 A | 14.2879 ± 0.0807 | 187.057 ± 0.151 | −69.591 ± 0.116 | 0.418 | 41 | 13.3090 ± 0.0009 | $0.5668^{+0.0884}_{-0.0824}$ | SHC |
| HD 23472 A* | 25.5897 ± 0.0261 | −102.571 ± 0.050 | −43.917 ± 0.059 | — | — | 9.3848 ± 0.0002 | $0.0783^{+0.1742}_{-0.0703}$ | |
| HD 23472 B | 25.5060 ± 0.0732 | −103.019 ± 0.154 | −42.771 ± 0.169 | 0.490 | 16.1 | 15.8312 ± 0.0014 | | |
| HD 24085 B* | 18.1859 ± 0.0245 | − 9.249 ± 0.048 | −97.358 ± 0.050 | — | — | 7.4250 ± 0.0002 | | |
| HD 24085 A | 18.1430 ± 0.0226 | −10.234 ± 0.043 | −97.151 ± 0.049 | — | — | 7.2719 ± 0.0002 | $0.6682^{+0.5911}_{-0.3903}$ | |
| HII 1348 A* (SB) | 6.9890 ± 0.0490 | 21.401 ± 0.120 | −45.705 ± 0.060 | — | — | 12.2439 ± 0.0012 | | |
| HII 1348 C | 6.6456 ± 0.1763 | 20.250 ± 0.337 | −45.292 ± 0.235 | 0.429 | 4.1 | 17.0303 ± 0.0017 | $1.1810^{+0.3091}_{-0.3321}$ | |
| HII 1348 D | 7.8946 ± 1.7831 | 23.361 ± 4.630 | −42.219 ± 2.330 | 2.369 | 0.9 | 20.7790 ± 0.0151 | $0.6550^{+0.3718}_{-0.4581}$ | |
| HATS-57 A* | 3.5495 ± 0.0392 | −12.664 ± 0.046 | −14.115 ± 0.040 | — | — | 12.1816 ± 0.0007 | $0.0548^{+0.1726}_{-0.0423}$ | |
| HATS-57 B | 3.4904 ± 0.1265 | −12.064 ± 0.174 | −14.764 ± 0.142 | — | — | 17.5558 ± 0.0012 | | |
| FU Tau A* | 7.5981 ± 0.1497 | 6.895 ± 0.376 | −21.026 ± 0.202 | 0.732 | 83 | 15.2412 ± 0.0024 | $2.2620^{+0.2597}_{-0.4841}$ | |
| FU Tau B | 7.4909 ± 1.2887 | 12.450 ± 4.056 | −21.761 ± 1.903 | 3.516 | 4.6 | 20.4799 ± 0.0074 | | |
| DH Tau A* | 7.3880 ± 0.0693 | 7.065 ± 0.117 | −20.699 ± 0.079 | — | — | 12.4961 ± 0.0090 | | |
| DH Tau C | 7.4011 ± 0.0520 | 6.899 ± 0.113 | −21.207 ± 0.074 | — | — | 11.9692 ± 0.0013 | $2.6683^{+0.3698}_{-0.1714}$ | |
| 51 Eri A* | 33.5770 ± 0.1354 | 44.352 ± 0.227 | −63.833 ± 0.178 | 0.562 | 190 | 5.1224 ± 0.0017 | $0.1740^{+0.2663}_{-0.1123}$ | |
| 51 Eri B (SB) | 37.9633 ± 0.3662 | 59.587 ± 0.717 | −52.419 ± 0.618 | 1.958 | 2030 | 9.7247 ± 0.0011 | | |
| 2M 0441+23 C* | 8.3040 ± 0.3778 | 8.955 ± 0.931 | −21.431 ± 0.456 | 1.350 | 5.7 | 18.9668 ± 0.0068 | | |
| 2M 0441+23 AB | 8.0161 ± 0.0832 | 8.300 ± 0.189 | −21.553 ± 0.103 | 0.529 | 79 | 13.8267 ± 0.0011 | $1.0577^{+0.9503}_{-0.4138}$ | |
| NGTS-6 A* | 3.2151 ± 0.0148 | − 9.339 ± 0.025 | −21.9950 ± 0.026 | — | — | 13.8175 ± 0.0006 | | |
| NGTS-6 B | 3.2231 ± 0.0653 | − 9.301 ± 0.107 | −22.1300 ± 0.114 | 0.203 | 1.3 | 17.0603 ± 0.0009 | $0.3627^{+0.1024}_{-0.1403}$ | |
| AB Dor AC* | 65.3199 ± 0.1440 | 29.150 ± 0.251 | 164.4210 ± 0.299 | 0.850 | 317 | 6.6738 ± 0.0018 | | |
| AB Dor BD | 67.0283 ± 0.0901 | 66.366 ± 0.155 | 125.8990 ± 0.189 | 0.522 | 111 | 11.3560 ± 0.0012 | $1.3528^{+0.5192}_{-0.4435}$ | |
| HD 39855 A* | 42.9636 ± 0.0346 | 92.854 ± 0.046 | −24.4660 ± 0.063 | — | — | 7.3211 ± 0.0002 | | |
| HD 39855 B | 42.9612 ± 0.0369 | 96.166 ± 0.055 | −11.8960 ± 0.065 | — | — | 10.0503 ± 0.0006 | $0.1920^{+0.2268}_{-0.1257}$ | |
| NGTS-10 A* | 3.0798 ± 0.2610 | − 2.323 ± 0.343 | 10.5270 ± 0.395 | 2.152 | 1,100 | 14.2604 ± 0.0034 | | |
| NGTS-10 B | 0.2965 ± 0.0802 | − 1.120 ± 0.219 | 9.6710 ± 0.161 | 0.064 | 0.3 | 15.5926 ± 0.0014 | $0.7679^{+1.1986}_{-0.5770}$ | SHC |
| L2 Pup A* | 15.61 ± 0.99 | 106.31 ± 0.96 | 324.99 ± 1.08 | — | — | 9.8208 ± 0.2812 | | HIP |
| L2 Pup B | 16.4131 ± 0.0574 | 105.895 ± 0.097 | 327.272 ± 0.099 | 0.368 | 12 | 15.7099 ± 0.0009 | $0.2940^{+0.3029}_{-0.0934}$ | |
| HIP 38594 A* | 56.1868 ± 0.0297 | −300.905 ± 0.044 | 200.923 ± 0.045 | — | — | 9.0853 ± 0.0003 | | |
| HIP 38594 B | 56.1234 ± 0.0799 | −297.867 ± 0.126 | 206.598 ± 0.257 | — | — | 16.0444 ± 0.0005 | $0.3670^{+0.7758}_{-0.2630}$ | |
| WASP-180 A* | 3.9093 ± 0.0517 | −14.052 ± 0.091 | − 3.169 ± 0.055 | — | — | 10.9134 ± 0.0007 | | |
| WASP-180 B | 3.8618 ± 0.0734 | −12.705 ± 0.172 | − 2.710 ± 0.103 | — | — | 11.7712 ± 0.0008 | $0.0930^{+0.1560}_{-0.0534}$ | |
| HD 79211 B* | 157.8851 ± 0.0414 | −1573.120 ± 0.061 | −660.121 ± 0.058 | — | — | 7.0477 ± 0.0004 | | |
| HD 79211 A | 157.8796 ± 0.0366 | −1546.100 ± 0.059 | −569.127 ± 0.060 | — | — | 6.9689 ± 0.0005 | $0.3757^{+0.3264}_{-0.2078}$ | |
| HD 85628 A* | 5.8297 ± 0.0318 | 6.051 ± 0.055 | −15.398 ± 0.051 | — | — | 8.1740 ± 0.0004 | $0.5012^{+0.1438}_{-0.2262}$ | |
| HD 85628 B | 5.9508 ± 0.0366 | 5.856 ± 0.066 | −13.252 ± 0.060 | 0.296 | 18 | 14.0490 ± 0.0047 | | |
| TOI 717 A* | 28.7709 ± 0.0783 | −26.092 ± 0.176 | 62.064 ± 0.260 | 0.045 | 0.5 | 12.6410 ± 0.0005 | $0.3110^{+0.1274}_{-0.0211}$ | |
| TOI 717 B | 28.7588 ± 0.0824 | −23.995 ± 0.177 | 62.081 ± 0.273 | 0.060 | 1.0 | 12.7386 ± 0.0008 | | |
| G 196-3 A* | 45.8611 ± 0.0388 | −141.177 ± 0.055 | −202.394 ± 0.053 | 0.000 | 0.5 | 10.6123 ± 0.0005 | $1.0645^{+0.4919}_{-0.4836}$ | |
| G 196-3 B | 44.3549 ± 0.8128 | −137.820 ± 0.928 | −208.523 ± 1.671 | 2.210 | 3.3 | 20.1697 ± 0.0085 | | |
| LTT 3780 A* | 45.4644 ± 0.0827 | −341.409 ± 0.114 | −247.870 ± 0.105 | 0.137 | 6.6 | 11.8465 ± 0.0005 | $0.5015^{+0.2595}_{-0.3436}$ | |
| LTT 3780 B | 45.2879 ± 0.1081 | −341.379 ± 0.149 | −248.419 ± 0.135 | 0.414 | 23 | 14.4855 ± 0.0008 | | |
| MASCARA-3 A* | 10.3320 ± 0.0333 | −56.184 ± 0.053 | −34.808 ± 0.064 | — | — | 8.2375 ± 0.0004 | $0.2400^{+0.2740}_{-0.1150}$ | |
| MASCARA-3 B | 11.0260 ± 0.1268 | −50.757 ± 0.325 | −37.811 ± 0.200 | 0.799 | 160 | 13.0002 ± 0.0109 | | |
| 2M J1101-7732 A* | 5.4081 ± 0.1877 | −22.653 ± 0.435 | 2.062 ± 0.397 | 1.271 | 12 | 18.3299 ± 0.0023 | | |
| 2M J1101-7732 B | 5.4333 ± 0.3368 | −23.668 ± 0.748 | 1.931 ± 0.723 | 1.836 | 6.1 | 19.4040 ± 0.0047 | $0.5900^{+0.1200}_{-0.1200}$ | ✠ |
| WASP-175 A* | 1.8260 ± 0.0399 | −24.306 ± 0.057 | 6.033 ± 0.057 | — | — | 12.7065 ± 0.0002 | | |
| WASP-175 B | 1.7947 ± 0.0308 | −24.064 ± 0.045 | 6.185 ± 0.045 | — | — | 14.2462 ± 0.0003 | $0.0965^{+0.0966}_{-0.0876}$ | |
| CHXR 73 A* | 5.2343 ± 0.1759 | −22.193 ± 0.233 | 0.215 ± 0.206 | 0.815 | 12 | 17.2934 ± 0.0014 | $3.4650^{+1.0250}_{-1.0250}$ | ✠ |
| CHXR 73 C | 5.2502 ± 0.2218 | −22.937 ± 0.433 | − 1.261 ± 0.347 | 1.241 | 14 | 17.9098 ± 0.0021 | | |

(Continued on following page)

**TABLE 2 |** (*Continued*) Gaia astro- and photometry of all exoplanet hosts and their companions, detected in this study.

| **Name** | $\pi$ **(mas)** | $\mu_\alpha \cos(\delta)$ **(mas/yr)** | $\mu_\delta$ **(mas/yr)** | **epsi (mas)** | **sig-epsi** | **G (mag)** | $A_G$ **(mag)** | |
|---|---|---|---|---|---|---|---|---|
| GJ 414 A* | 84.0803 ± 0.0471 | 591.622 ± 0.081 | −197.247 ± 0.091 | — | — | 7.7281 ± 0.0007 | | |
| GJ 414 B | 84.1971 ± 0.0579 | 604.831 ± 0.081 | −206.442 ± 0.075 | — | — | 9.0471 ± 0.0011 | $0.6100^{+0.5656}_{-0.3221}$ | |
| HD 97334 A* | 44.1428 ± 0.0383 | −249.387 ± 0.090 | −151.590 ± 0.071 | — | — | 6.2410 ± 0.0006 | $0.0555^{+0.1848}_{-0.0415}$ | |
| HD 97334 BC | 42.8724 ± 1.1025 | −236.349 ± 2.133 | −152.068 ± 2.109 | 5.342 | 15 | 19.9859 ± 0.0135 | | |
| HD 233832 A* | 16.9952 ± 0.0752 | −473.960 ± 0.075 | 124.167 ± 0.087 | — | — | 9.9456 ± 0.0005 | | |
| HD 233832 B | 17.0667 ± 0.0532 | −478.645 ± 0.048 | 119.122 ± 0.088 | — | — | 12.7187 ± 0.0004 | $0.2288^{+0.2054}_{-0.1079}$ | |
| 2M J1155-7919 A* | 9.8862 ± 0.0585 | −41.179 ± 0.127 | − 4.336 ± 0.086 | 0.490 | 35 | 14.8180 ± 0.0017 | $0.4158^{+0.0616}_{-0.0052}$ | ✠ |
| 2M J1155-7919 B | 9.8211 ± 0.5264 | −39.738 ± 1.216 | − 4.656 ± 0.687 | 1.387 | 1.4 | 19.9246 ± 0.0079 | | |
| NGTS-5 A* | 3.2310 ± 0.0272 | 13.650 ± 0.041 | − 4.688 ± 0.042 | — | — | 13.5260 ± 0.0004 | $0.1970^{+0.1050}_{-0.1174}$ | |
| NGTS-5 B | 2.9428 ± 0.1254 | 13.938 ± 0.209 | − 4.331 ± 0.180 | 0.422 | 3.0 | 17.3160 ± 0.0016 | | |
| 2M J1450-7841 A* | 10.9480 ± 0.5046 | −37.597 ± 0.881 | −23.654 ± 0.895 | 2.345 | 5.0 | 19.6858 ± 0.0060 | $0.5000^{+0.5000}_{-0.5000}$ | ✠ |
| 2M J1450-7841 B | 8.6592 ± 0.9023 | −34.984 ± 2.047 | −22.162 ± 1.764 | 2.067 | 1.1 | 20.6501 ± 0.0097 | | |
| WASP-189 A* | 9.9990 ± 0.0747 | −50.564 ± 0.109 | −23.788 ± 0.115 | 0.082 | 2.2 | 6.5537 ± 0.0004 | $0.2652^{+0.1599}_{-0.2306}$ | SHC |
| WASP-189 B | 10.7202 ± 0.1648 | −50.594 ± 0.165 | −24.037 ± 0.178 | 0.475 | 25 | 14.3874 ± 0.0024 | | |
| HIP 73990 A* | 9.0326 ± 0.0648 | −27.432 ± 0.106 | −29.028 ± 0.089 | — | — | 8.0678 ± 0.0009 | | |
| HIP 73990 D | 8.9507 ± 0.0899 | −27.728 ± 0.159 | −29.245 ± 0.135 | 0.457 | 28 | 14.6580 ± 0.0007 | $1.1073^{+0.6427}_{-0.4489}$ | |
| TOI 905 A* | 6.2745 ± 0.0285 | −25.839 ± 0.033 | −41.150 ± 0.051 | — | — | 11.0813 ± 0.0004 | $0.2703^{+0.1330}_{-0.1606}$ | SHC |
| TOI 905 B | 7.8542 ± 0.5489 | −18.290 ± 0.763 | −39.819 ± 0.788 | 1.423 | 25 | 17.2149 ± 0.0375 | | |
| 2M 1510 A* | 27.2203 ± 0.2665 | −118.747 ± 0.492 | −46.865 ± 0.420 | 1.112 | 18 | 17.4870 ± 0.0018 | $0.9266^{+0.1360}_{-0.0121}$ | SHC |
| 2M 1510 B | 27.6869 ± 0.4939 | −117.448 ± 0.893 | −45.713 ± 0.746 | 1.710 | 7.8 | 18.8855 ± 0.0035 | | |
| β Cir A* | 35.1736 ± 0.4253 | −96.742 ± 0.491 | −136.541 ± 0.621 | 1.852 | 1770 | 3.9732 ± 0.0026 | $0.2560^{+0.2260}_{-0.1598}$ | |
| β Cir B | 34.7836 ± 0.6840 | −92.763 ± 0.829 | −138.156 ± 1.469 | 2.701 | 15 | 19.4335 ± 0.0051 | | |
| KELT-23 A* | 7.8912 ± 0.0219 | 0.434 ± 0.039 | −12.217 ± 0.041 | — | — | 10.1820 ± 0.0004 | $0.0680^{+0.0996}_{-0.0505}$ | |
| KELT-23 B | 7.8949 ± 0.0529 | 1.567 ± 0.093 | −11.903 ± 0.107 | 0.284 | 6.8 | 15.5209 ± 0.0014 | | |
| K2-290 A*B | 3.6365 ± 0.0503 | 27.225 ± 0.099 | −16.893 ± 0.066 | — | — | 10.8204 ± 0.0004 | $0.8900^{+0.2570}_{-0.2655}$ | |
| K2-290 C | 4.0531 ± 0.2711 | 27.465 ± 0.593 | −16.484 ± 0.370 | 0.556 | 1.2 | 18.5920 ± 0.0027 | | |
| GQ Lup A* | 6.5868 ± 0.0473 | −14.257 ± 0.097 | −23.596 ± 0.066 | 0.110 | 5.7 | 11.2608 ± 0.0089 | $2.7645^{+0.3426}_{-0.4140}$ | |
| GQ Lup C | 5.4925 ± 0.4597 | −14.807 ± 0.972 | −21.947 ± 0.653 | 2.960 | 59 | 18.3740 ± 0.0037 | | |
| HIP 77900 A* | 6.6037 ± 0.1196 | −13.357 ± 0.187 | −25.272 ± 0.110 | 0.212 | 21 | 6.1129 ± 0.0006 | $0.1852^{+0.1535}_{-0.0360}$ | |
| HIP 77900 B | 5.2279 ± 0.9696 | −13.908 ± 1.517 | −23.265 ± 1.097 | 2.007 | 4.3 | 19.5660 ± 0.0057 | | |
| USco 1602-2401 A* | 6.9484 ± 0.0661 | −11.850 ± 0.119 | −24.032 ± 0.051 | — | — | 11.8656 ± 0.0026 | $1.8885^{+0.1123}_{-0.1186}$ | SHC |
| USco 1602-2401 B | 6.3381 ± 0.2030 | −12.699 ± 0.325 | −23.872 ± 0.187 | 0.829 | 40 | 16.3640 ± 0.0010 | | |
| HIP 79098 A (SB)* | 6.8337 ± 0.1176 | − 9.823 ± 0.210 | −28.119 ± 0.163 | 0.289 | 35 | 5.8264 ± 0.0006 | $0.4640^{+0.1440}_{-0.2381}$ | |
| HIP 79098 C | 7.1870 ± 0.1476 | −10.979 ± 0.271 | −26.128 ± 0.189 | 0.666 | 27 | 16.1091 ± 0.0012 | | |
| USco 1610-1913 A* | 7.4960 ± 0.0718 | − 9.342 ± 0.206 | −23.591 ± 0.111 | 0.168 | 12 | 12.6962 ± 0.0049 | $0.3850^{+0.3850}_{-0.3850}$ | ✠ |
| USco 1610-1913 B | 6.9600 ± 0.3719 | − 7.043 ± 1.112 | −24.982 ± 0.576 | 1.301 | 7.0 | 18.7225 ± 0.0029 | | |
| USco 1612-1800 A* | 6.3156 ± 0.0747 | − 7.418 ± 0.161 | −21.148 ± 0.112 | 0.427 | 31 | 14.5532 ± 0.0007 | $0.3850^{+0.3850}_{-0.3850}$ | ✠ |
| USco 1612-1800 B | 6.0413 ± 0.3224 | − 7.002 ± 0.698 | −19.738 ± 0.512 | 1.112 | 4.0 | 18.8810 ± 0.0032 | | |
| ROXs 12 A* | 7.2894 ± 0.0417 | − 7.185 ± 0.090 | −24.851 ± 0.059 | 0.158 | 6.9 | 13.2655 ± 0.0013 | $1.8000^{+1.0000}_{-1.0000}$ | ✠ |
| ROXs 12 C | 7.2328 ± 0.0738 | − 6.577 ± 0.151 | −25.106 − 0:099 | 0.354 | 20 | 14.7659 ± 0.0113 | | |
| HATS-48 A* | 3.7648 ± 0.0237 | 3.125 ± 0.031 | 6.146 ± 0.029 | — | — | 13.8951 ± 0.0002 | $0.5090^{+0.1876}_{-0.3705}$ | |
| HATS-48 B | 3.6354 ± 0.4432 | 2.951 ± 0.469 | 5.201 ± 0.446 | 0.576 | 0.6 | 19.3368 ± 0.0037 | | |
| GJ 752 A* | 169.1590 ± 0.0520 | −579.043 ± 0.088 | −1332.740 ± 0.081 | — | — | 8.0976 ± 0.0011 | | |
| GJ 752 B | 168.9620 ± 0.1299 | −598.177 ± 0.245 | −1365.270 ± 0.227 | 0.855 | 98 | 14.3212 ± 0.0007 | $1.4208^{+0.2795}_{-0.1719}$ | |
| HD 181234 A* | 20.9155 ± 0.0564 | −122.751 ± 0.098 | −318.277 ± 0.098 | — | — | 8.3693 ± 0.0004 | $0.3670^{+0.1987}_{-0.0723}$ | |
| HD 181234 B | 20.8683 ± 0.1458 | −117.558 ± 0.192 | −323.292 ± 0.211 | 0.520 | 27 | 14.2207 ± 0.0012 | | |
| Wendelstein-1 A* | 3.2470 ± 0.0317 | 4.131 ± 0.041 | − 1.832 ± 0.039 | — | — | 15.0324 ± 0.0005 | $0.5240^{+0.4730}_{-0.4315}$ | |
| Wendelstein-1 B | 3.5833 ± 0.4053 | 3.862 ± 0.508 | − 2.194 ± 0.536 | 1.038 | 1.9 | 19.3979 ± 0.0031 | | |
| 2M J2126-81 A* | 29.2836 ± 0.0690 | 59.843 ± 0.111 | −107.723 ± 0.114 | 0.303 | 48 | 10.8133 ± 0.0021 | $0.2157^{+0.4319}_{-0.0470}$ | SHC |
| 2M J2126-81 B | 29.2463 ± 0.9205 | 56.511 ± 1.656 | −115.369 ± 2.441 | 4.299 | 4.4 | 20.7247 ± 0.0094 | | |
| TOI 132 A* | 6.0809 ± 0.0366 | 35.553 ± 0.043 | −53.055 ± 0.054 | 0.090 | 3.6 | 11.3208 ± 0.0007 | $0.1535^{+0.1606}_{-0.1430}$ | |
| TOI 132 B | 5.9683 ± 0.2251 | 35.417 ± 0.280 | −52.488 ± 0.361 | 0.955 | 7.4 | 18.4470 ± 0.0015 | | |
| NGTS-7 A* | 7.2497 ± 0.1203 | −27.003 ± 0.114 | −16.225 ± 0.178 | 0.610 | 72 | 14.9154 ± 0.0020 | $0.5000^{+0.5000}_{-0.5000}$ | ✠ |
| NGTS-7 B | 6.5232 ± 0.0787 | −28.601 ± 0.112 | −14.776 ± 0.364 | 0.203 | 4.4 | 15.5134 ± 0.0012 | | |
| DS Tuc A* | 22.6663 ± 0.0354 | 79.464 ± 0.074 | −67.440 ± 0.045 | — | — | 8.3193 ± 0.0010 | | |
| DS Tuc B | 22.6504 ± 0.0297 | 78.022 ± 0.064 | −65.746 ± 0.037 | — | — | 9.3993 ± 0.0014 | $0.3210^{+0.2350}_{-0.1034}$ | |
| 1RXS J2351+3127 A* | 23.2183 ± 0.0524 | 106.584 ± 0.064 | −87.761 ± 0.038 | 0.083 | 3.9 | 12.5145 ± 0.0005 | | |
| 1RXS J2351+3127 C | 23.1794 ± 0.0592 | 105.757 ± 0.070 | −87.787 ± 0.041 | 0.285 | 32 | 13.2004 ± 0.0006 | $0.4190^{+0.4250}_{-0.0410}$ | |

*Comments on individual objects:*

*HD 1160 A hosts a brown dwarf companion (HD 1160 B, detected by Nielsen et al., 2012), which is listed as exoplanet in the EPE.*

*The exoplanet host star HD 24085 B is the secondary component of a binary system, whose primary star HD 24085 A is also known as HD 24062.*

*HII 1348 A is a spectroscopic binary with a brown dwarf companion (HII 1348 B, discovered by Geißler et al., 2012), which is listed as exoplanet in the EPE.*

*DH Tau A hosts a brown dwarf companion (DH Tau B), which was detected by Itoh et al. (2005) and is listed as exoplanet in the EPE. DH Tau C (alias DI Tau) is the wide primary component of this system.*

*2M 0441+23 C is an exoplanet host brown dwarf (Bowler and Hillenbrand, 2015), which is listed in the EPE.*
*The bright AGB star L2 Pup A is listed in the Gaia DR2 but with a parallax (π = 7.3644 ± 0.6149 mas) that significantly differs from its HIPPARCOS-value (π = 15.61 ± 0.99 mas, van Leeuwen, 2007). Furthermore, it should be noted that the G-band brightness of this star, as listed in the Gaia DR2, is several magnitudes fainter than expected (e.g. G = 3.97 ± 0.54 mag, as estimated by Smart and Nicastro, 2014). Therefore, we only use here the Gaia DR2 equatorial coordinates of this star, while we adopt the HIPPARCOS-values of its parallax and proper motion, which is indicated with the flag HIP in this table.*
*HIP 73990 A is the host star of two brown dwarfs (HIP 73990 B and C, revealed by Hinkley et al., 2015), which are both listed as exoplanets in the EPE.*
*GQ Lup A is listed as exoplanet host star in the EPE, whose substellar companion was detected by Neuhäuser et al. (2005). The star exhibits a wide stellar companion, whose WDS designation (GQ Lup C) is used here.*
*HIP 79098 A is a spectroscopic binary and hosts the brown dwarf HIP 79098 B (Janson et al., 2019), which is listed as exoplanet in the EPE.*
*ROXs 12 A is the host star of the brown dwarf ROXs 12 B, detected by Kraus et al. (2014), which is listed as exoplanet in the EPE.*
*1RXS J2351+3127 A hosts a brown dwarf companion (1RXS J2351+3127 B, discovered by Bowler et al., 2012), which is listed as exoplanet in the EPE.*
*HII 1348 A, FU Tau A, G 196-3 A, 2M J1155-7919 A, HD 97334 A, β Cir A, HIP 77900 A, USco 1602-2401 A, USco 1610-1913 A, USco 1612-1800 A, and 2M J2126-81 A, are all listed as exoplanet host stars in the EPE, whose substellar companions were detected and characterized in this study, using data from the Gaia DR2.*
*2M J1101-7732 A, 2M J1450-7841 A, 2M 1510 A are all brown dwarfs, which are listed as exoplanet hosts in the EPE, whose substellar companions were detected and characterized in this study with Gaia DR2 data.*

i.e. the sum of the mass of the companions, derived as described above, and the mass of the associated exoplanet hosts, taken from the EPE. This estimation can be considered as an upper limit of the escape velocity as the projected separation is smaller than the physical separation of the objects.

## 3 DETECTED COMPANIONS OF EXOPLANET HOSTS

The Gaia astro- and photometry of all exoplanet hosts and their companions, detected in this study, are listed in **Table 2**. The derived properties of the companions are summarized in **Table 3–5**. In all tables the exoplanet host systems or the companions are sorted by their right ascension. The used identifier of the targets corresponds either to the one used in the EPE or is a slightly abbreviated version of it. In contrast to the planet definition used by the EPE, in which substellar objects below 60 $M_{\mathrm{Jup}}$ are defined as exoplanets, we follow here the planet definition based on the deuterium burning limit (as described e.g. by Basri, 2000), i.e. all substellar objects below 13 $M_{\mathrm{Jup}}$ are classified as exoplanets, while more massive objects below the substellar/stellar mass limit (at about 0.072 $M_{\odot}$ for solar metallicity) as brown dwarfs, respectively. Thereby the given masses of the exoplanets, detected by radial velocity measurements, correspond to minimum-masses ($M\sin(i)$) due to the unknown orbital inclination, while masses of direct imaging planets are usually derived from their spectrophotometry with evolutionary models.

In **Table 2** for each exoplanet host and its detected co-moving companion(s) their Gaia DR2 parallax π, proper motion in right ascension and declination ($\mu_{\alpha}\cos(\delta)$ and $\mu_{\delta}$), astrometric excess noise (epsi) with its significance (sig-epsi), apparent G-band magnitude, as well as the used Apsis-Priam G-band extinction estimate $A_G$ are listed. In the case that the G-band extinction was taken from the StarHorse catalog this is indicated with the SHC flag, or with the ✠ flag if the G-band extinction was derived from V-band extinction measurements, either listed in the VizieR database or from the literature. In this table the exoplanet hosts are indicated with *, and known spectroscopic binary stars among them with (SB).

**Table 3** lists for each detected companion its angular separation (ρ) and position angle (PA) to the associated exoplanet host, which were determined with the Gaia DR2 astrometry of the objects for the (Gaia reference) epoch 2015.5. The relative astrometry of the companions exhibits an uncertainty on average of 0.3 mas in angular separation, and 0.002° in position angle, respectively. In the following columns of **Table 3** we list the parallax difference ($\Delta\pi$) with its significance (in brackets calculated by taking into account also the Gaia astrometric excess noise[3]) between the exoplanet hosts and their detected companions, their differential proper motion $\mu_{\mathrm{rel}}$ with its significance, and the cpm-index of all systems. The precise Gaia DR2 astrometry proves the equidistance (sig-$\Delta\pi < 2.3\sigma$, average value of $0.5\sigma$) and common proper motion ($\mathrm{cpm-index} > 6$, $\mathrm{average\ cpm-index} = 118$) of the exoplanet hosts and their companions. If these companions are not listed yet as companion (-candidates) in the Washington Double Star Catalog (WDS from hereon, Mason et al., 2001) this is indicated with the ★ flag in last column of **Table 3**. In the case that the companion is not listed in the WDS but was reported in literature before, additional information is given in the notes of this table.

In **Table 4** beside the equatorial coordinates (α, δ both for epoch 2015.5) of all detected companions, their derived absolute G-band magnitude $M_G$, projected separation *sep* to the associated exoplanet host (relative uncertainty about 1%, on average), mass, and effective temperature $T_{\mathrm{eff}}$ are summarized. The flags listed in the last column of this table are defined as follows:

- PRI: An Apsis-Priam temperature estimate is available for the detected companion, which could be compared with the effective temperature of the companion, derived from its absolute G-band photometry using the Baraffe et al. (2015) models.
- 2MA: The companion is listed in the 2MASS Point Source catalog.
- BPRP: The $G_{\mathrm{BP}} - G_{\mathrm{RP}}$ color of the exoplanet host and of the detected companion is listed in the Gaia DR2, hence a color comparison was feasible.
- EXT: Because of its brightness the companion exceeds the magnitude range of the Baraffe et al. (2015) evolutionary

[3]The astrometric excess noise is conservatively considered here as additional parallax uncertainty of the source.

**TABLE 3 |** The relative astrometry and WDS status of all detected companions.

| Companion | ρ (arcsec) | PA (°) | $\Delta\pi$ (mas) | sig-$\Delta\pi$ | $\mu_{rel}$ (mas/yr) | sig-$\mu_{rel}$ | cpm-index | Not in WDS |
|---|---|---|---|---|---|---|---|---|
| HD 1160 C | 5.14549 ± 0.00018 | 349.53223 ± 0.00259 | 0.95 ± 0.28 | 3.3 (1.2) | 1.72 ± 0.33 | 5.2 | 30 | |
| Gliese 49 B | 294.45989 ± 0.00011 | 75.52728 ± 0.00002 | 0.17 ± 0.09 | 2.0 (0.8) | 4.36 ± 0.23 | 19 | 338 | |
| HD 8326 B | 56.88131 ± 0.00005 | 147.16909 ± 0.00006 | 0.12 ± 0.08 | 1.6 (0.3) | 1.18 ± 0.17 | 7.1 | 394 | |
| HD 13167 B | 20.06421 ± 0.00010 | 24.77589 ± 0.00028 | 0.11 ± 0.13 | 0.8 (0.2) | 1.28 ± 0.23 | 5.7 | 91 | ★ |
| HR 858 B | 8.35742 ± 0.00013 | 15.79337 ± 0.00060 | 1.04 ± 0.18 | 5.8 (1.2) | 13.90 ± 0.22 | 62 | 24 | ★ |
| HD 18015 B | 7.08916 ± 0.00006 | 316.16832 ± 0.00045 | 0.11 ± 0.07 | 1.6 (1.6) | 1.61 ± 0.11 | 14 | 79 | |
| K2-288 A | 0.78692 ± 0.00018 | 340.38240 ± 0.01437 | 0.93 ± 0.22 | 4.3 (1.0) | 4.75 ± 0.64 | 7.4 | 84 | ★[b] |
| HD 23472 B | 9.56924 ± 0.00008 | 45.28294 ± 0.00046 | 0.08 ± 0.08 | 1.1 (0.2) | 1.23 ± 0.18 | 7.0 | 181 | ★ |
| HD 24085 A | 75.91260 ± 0.00003 | 263.05666 ± 0.00002 | 0.04 ± 0.03 | 1.3 (1.3) | 1.01 ± 0.06 | 16 | 194 | ★ |
| HII 1348 C | 36.02849 ± 0.00016 | 276.87735 ± 0.00017 | 0.34 ± 0.18 | 1.9 (0.7) | 1.22 ± 0.35 | 3.5 | 82 | ★ |
| HII 1348 D | 55.01726 ± 0.00090 | 182.06892 ± 0.00182 | 0.91 ± 1.78 | 0.5 (0.3) | 4.00 ± 3.05 | 1.3 | 25 | ★ |
| HATS-57 B | 14.44086 ± 0.00010 | 282.25351 ± 0.00032 | 0.06 ± 0.13 | 0.4 (0.4) | 0.88 ± 0.16 | 5.4 | 43 | ★ |
| FU Tau B | 5.68952 ± 0.00112 | 123.57637 ± 0.00858 | 0.11 ± 1.30 | 0.1 (0.0) | 5.60 ± 4.05 | 1.4 | 8 | |
| DH Tau C | 15.29981 ± 0.00007 | 126.08805 ± 0.00023 | 0.01 ± 0.09 | 0.2 (0.2) | 0.53 ± 0.11 | 4.7 | 83 | |
| 51 Eri B (SB) | 66.96749 ± 0.00027 | 162.62918 ± 0.00028 | 4.39 ± 0.39 | 11.2 (2.1) | 19.04 ± 0.71 | 27 | 8 | |
| 2M 0441+23 AB | 12.31449 ± 0.00036 | 57.55273 ± 0.00133 | 0.29 ± 0.39 | 0.7 (0.2) | 0.67 ± 0.94 | 0.7 | 70 | |
| NGTS-6 B | 5.36108 ± 0.00005 | 116.68846 ± 0.00060 | 0.01 ± 0.07 | 0.1 (0.0) | 0.14 ± 0.12 | 1.2 | 342 | ★ |
| AB Dor BD | 8.87930 ± 0.00018 | 347.19358 ± 0.00097 | 1.71 ± 0.17 | 10.1 (1.7) | 53.56 ± 0.33 | 164 | 6 | |
| HD 39855 B | 10.72622 ± 0.00004 | 19.55064 ± 0.00017 | 0.00 ± 0.05 | 0.0 (0.0) | 13.00 ± 0.09 | 145 | 15 | |
| NGTS-10 B | 1.12234 ± 0.00023 | 334.73644 ± 0.01107 | 2.78 ± 0.27 | 10.2 (1.3) | 1.48 ± 0.41 | 3.6 | 14 | ★[c] |
| L2 Pup B | 32.80132 ± 0.00052 | 63.66528 ± 0.00099 | 0.80 ± 0.99 | 0.8 (−) | 2.32 ± 1.08 | 2.2 | 296 | ★ |
| HIP 38594 B | 399.81589 ± 0.00012 | 208.91546 ± 0.00001 | 0.06 ± 0.09 | 0.7 (0.7) | 6.44 ± 0.24 | 27 | 113 | |
| WASP-180 B | 4.86185 ± 0.00006 | 138.92126 ± 0.00081 | 0.05 ± 0.09 | 0.5 (0.5) | 1.42 ± 0.19 | 7.6 | 19 | |
| HD 79211 A | 17.08255 ± 0.00004 | 277.72812 ± 0.00014 | 0.01 ± 0.06 | 0.1 (0.1) | 94.92 ± 0.08 | 1,136 | 35 | |
| HD 85628 B | 4.33622 ± 0.00004 | 224.93946 ± 0.00056 | 0.12 ± 0.05 | 2.5 (0.4) | 2.15 ± 0.08 | 27 | 14 | ★[d] |
| TOI 717 B | 65.46692 ± 0.00016 | 88.63021 ± 0.00020 | 0.01 ± 0.11 | 0.1 (0.1) | 2.10 ± 0.25 | 8.4 | 64 | |
| G 196-3 B | 16.06941 ± 0.00055 | 209.15563 ± 0.00166 | 1.51 ± 0.81 | 1.9 (0.6) | 6.99 ± 1.53 | 4.6 | 71 | |
| LTT 3780 B | 15.78849 ± 0.00011 | 97.14133 ± 0.00038 | 0.18 ± 0.14 | 1.3 (0.4) | 0.55 ± 0.17 | 3.2 | 1,535 | |
| MASCARA-3 B | 2.06449 ± 0.00010 | 173.15273 ± 0.00345 | 0.69 ± 0.13 | 5.3 (0.9) | 6.20 ± 0.31 | 20 | 21 | ★[e] |
| 2M J1101-7732 B | 1.42656 ± 0.00041 | 30.00553 ± 0.01621 | 0.03 ± 0.39 | 0.1 (0.0) | 1.02 ± 0.86 | 1.2 | 45 | |
| WASP-175 B | 7.25020 ± 0.00003 | 4.95541 ± 0.00027 | 0.03 ± 0.05 | 0.6 (0.6) | 0.29 ± 0.07 | 3.9 | 175 | ★[f] |
| CHXR 73 C | 46.10344 ± 0.00027 | 248.30821 ± 0.00031 | 0.02 ± 0.28 | 0.1 (0.0) | 1.65 ± 0.42 | 3.9 | 27 | ★ |
| GJ 414 B | 34.15873 ± 0.00007 | 262.44625 ± 0.00011 | 0.12 ± 0.07 | 1.6 (1.6) | 16.09 ± 0.12 | 139 | 78 | |
| HD 97334 BC | 89.88421 ± 0.00098 | 245.04583 ± 0.00060 | 1.27 ± 1.10 | 1.2 (0.2) | 13.05 ± 2.13 | 6.1 | 44 | |
| HD 233832 B | 4.93691 ± 0.00004 | 266.38672 ± 0.00079 | 0.07 ± 0.09 | 0.8 (0.8) | 6.88 ± 0.11 | 63 | 143 | |
| 2M J1155-7919 B | 5.75435 ± 0.00047 | 227.86140 ± 0.00458 | 0.07 ± 0.53 | 0.1 (0.0) | 1.48 ± 1.20 | 1.2 | 55 | ★[g] |
| NGTS-5 B | 26.89147 ± 0.00011 | 116.31597 ± 0.00021 | 0.29 ± 0.13 | 2.2 (0.7) | 0.46 ± 0.20 | 2.3 | 63 | ★ |
| 2M J1450-7841 B | 4.23901 ± 0.00099 | 313.26065 ± 0.01318 | 2.29 ± 1.03 | 2.2 (0.7) | 3.01 ± 2.17 | 1.4 | 29 | ★[h] |
| WASP-189 B | 9.41610 ± 0.00010 | 70.78901 ± 0.00095 | 0.72 ± 0.18 | 4.0 (1.4) | 0.25 ± 0.21 | 1.2 | 446 | ★ |
| HIP 73990 D | 47.27427 ± 0.00009 | 56.65125 ± 0.00010 | 0.08 ± 0.11 | 0.7 (0.2) | 0.37 ± 0.18 | 2.0 | 219 | ★ |
| TOI 905 B | 2.24803 ± 0.00050 | 100.34253 ± 0.01658 | 1.58 ± 0.55 | 2.9 (1.0) | 7.67 ± 0.76 | 10 | 12 | |
| 2M 1510 B | 6.77139 ± 0.00046 | 209.28499 ± 0.00431 | 0.47 ± 0.56 | 0.8 (0.2) | 1.74 ± 0.95 | 1.8 | 146 | ★[i] |
| β Cir B | 217.62247 ± 0.00055 | 199.25875 ± 0.00013 | 0.39 ± 0.81 | 0.5 (0.1) | 4.29 ± 1.08 | 4.0 | 78 | |
| KELT-23 B | 4.54135 ± 0.00006 | 127.68919 ± 0.00069 | 0.00 ± 0.06 | 0.1 (0.0) | 1.18 ± 0.10 | 12 | 21 | ★[j] |
| K2-290 C | 11.25119 ± 0.00017 | 179.97609 ± 0.00151 | 0.42 ± 0.28 | 1.5 (0.7) | 0.47 ± 0.44 | 1.1 | 135 | ★[k] |
| GQ Lup C | 16.11286 ± 0.00039 | 114.61327 ± 0.00099 | 1.09 ± 0.46 | 2.4 (0.4) | 1.74 ± 0.70 | 2.5 | 31 | |
| HIP 77900 B | 22.27990 ± 0.00044 | 12.74996 ± 0.00267 | 1.38 ± 0.98 | 1.4 (0.6) | 2.08 ± 1.14 | 1.8 | 27 | ★[l] |
| USco 1602-2401 B | 7.21512 ± 0.00008 | 353.20771 ± 0.00157 | 0.61 ± 0.21 | 2.9 (0.7) | 0.86 ± 0.34 | 2.5 | 62 | |
| HIP 79098 C | 65.29721 ± 0.00018 | 101.86730 ± 0.00008 | 0.35 ± 0.19 | 1.9 (0.5) | 2.30 ± 0.28 | 8.3 | 25 | ★[m] |
| USco 1610-1913 B | 5.82725 ± 0.00040 | 113.57990 ± 0.00238 | 0.54 ± 0.38 | 1.4 (0.4) | 2.69 ± 1.01 | 2.7 | 19 | |
| USco 1612-1800 B | 3.18438 ± 0.00019 | 10.65437 ± 0.00561 | 0.27 ± 0.33 | 0.8 (0.2) | 1.47 ± 0.54 | 2.7 | 29 | ★[n] |
| ROXs 12 C | 37.14026 ± 0.00004 | 185.99483 ± 0.00012 | 0.06 ± 0.08 | 0.7 (0.1) | 0.66 ± 0.17 | 3.9 | 79 | ★[o] |
| HATS-48 B | 5.43813 ± 0.00025 | 267.59024 ± 0.00322 | 0.13 ± 0.44 | 0.3 (0.2) | 0.96 ± 0.45 | 2.2 | 13 | ★[p] |
| GJ 752 B | 75.48951 ± 0.00011 | 152.49075 ± 0.00009 | 0.20 ± 0.14 | 1.4 (0.2) | 37.74 ± 0.25 | 153 | 78 | |
| HD 181234 B | 5.17023 ± 0.00011 | 56.61253 ± 0.00118 | 0.05 ± 0.16 | 0.3 (0.1) | 7.22 ± 0.22 | 32 | 95 | |
| Wendelstein-1 B | 11.79208 ± 0.00024 | 232.62838 ± 0.00116 | 0.34 ± 0.41 | 0.8 (0.3) | 0.45 ± 0.53 | 0.9 | 20 | ★ |
| 2M J2126-81 B | 217.49441 ± 0.00082 | 123.98914 ± 0.00024 | 0.04 ± 0.92 | 0.0 (0.0) | 8.34 ± 2.34 | 3.6 | 30 | |
| TOI 132 B | 19.64887 ± 0.00018 | 151.44437 ± 0.00044 | 0.11 ± 0.23 | 0.5 (0.1) | 0.58 ± 0.36 | 1.6 | 218 | ★ |
| NGTS-7 B | 1.13095 ± 0.00014 | 117.57142 ± 0.01072 | 0.73 ± 0.14 | 5.1 (1.1) | 2.16 ± 0.30 | 7.3 | 30 | ★[q] |
| DS Tuc B | 5.36461 ± 0.00003 | 347.65815 ± 0.00047 | 0.02 ± 0.05 | 0.3 (0.3) | 2.22 ± 0.08 | 29 | 93 | |
| 1RXS J2351+3127 C | 126.01641 ± 0.00005 | 98.50769 ± 0.00002 | 0.04 ± 0.08 | 0.5 (0.1) | 0.83 ± 0.09 | 8.7 | 333 | |

*Comments on individual companions:*

[a]*This companion was first reported by Vanderburg et al. (2019), who have already verified its equidistance and common proper motion with the exoplanet host star HR 858 A using Gaia DR2 data, consistent with the results, obtained in this study.*

[b]This companion was detected by Feinstein et al. (2019) and its companionship with the exoplanet host star K2-288 B was proven with Gaia DR2 astrometry, confirmed by the astrometric analysis, carried out in the study, presented here.
[c]This star was already noticed in the Gaia DR2 by McCormac et al. (2020) as common proper motion companion of the exoplanet host star NGTS-10 A, consistent with the results, derived in this study.
[d]This companion of the exoplanet host star HD 85628 A was discovered by Dorval et al. (2020) in the Gaia DR2, who found its parallax and proper motion consistent with that of the exoplanet host star, confirmed by the astrometric analysis, presented here.
[e]This companion was detected with AO imaging by Rodriguez et al. (2019) using Keck/NIRC 2, but is also listed in the Gaia DR2, whose astrometry was used by this team to verify the equidistance and common proper motion of this companion with the exoplanet host star MASCARA-3 A, as done in this study.
[f]This companion was already reported by Nielsen et al. (2019), who proved its companionship with the exoplanet host star WASP-175 A with Gaia DR2 astrometry, consistent with the results derived here.
[g]The equidistance and common proper motion of this substellar object with the exoplanet host star 2M J1155-7919 A was verified by Dickson-Vandervelde et al. (2020) using Gaia DR2 data, as done in this work.
[h]This companion was detected by Burgasser et al. (2017) and its common proper motion with the brown dwarf 2M J1450-7841 A, listed in the EPE, was verified with ground based astrometry, confirmed in this study with Gaia DR2 data, which furthermore proves the equidistance of both objects.
[i]This companion was noticed by Triaud et al. (2020) in the Gaia DR2 as equidistant and co-moving companion of the brown dwarf 2M 1510 A, which is listed in the EPE, consistent with our results.
[j]KELT-23 B was first discovered by (Johns et al., 2019) with Keck/NIRC2 AO imaging, who used Gaia DR2 astrometry to prove the equidistance and common proper motion of the companion with the exoplanet host star KELT-23 A, as done in this study.
[k]This companion was already described by Hjorth et al. (2019), who have verified it to be equidistant and co-moving with the exoplanet host star K2-290 A, using Gaia DR2 data, a conclusion, which is confirmed by the analysis, presented here. Furthermore, this team identified an additional but closer stellar companion-candidate of the exoplanet host star (K2-290 B) with Subrau/IRCS AO imaging, which however still needs astrometric confirmation of its companionship. Due to its close angular separation to K2-290 A we adopt here this object as companion of the exoplanet host star.
[l]This companion was revealed spectro-photometrically by Aller et al. (2013). With Gaia DR2 astrometry we prove here its companionship with the exoplanet host star HIP 77900 A.
[m]HIP 79098 C was reported by (Janson et al., 2019) as equidistant and co-moving companion of the exoplanet host star HIP 79098 A, based on its Gaia DR2 astrometry, confirmed by the analysis of the companion, which is presented here.
[n]This companion was revealed spectro-photometrically by Aller et al. (2013). The equidistance and common proper motion of this companion with the exoplanet host star USco 1612-1800 A was proven in this study, with Gaia DR2 astrometry.
[o]This star was identified by (Bowler et al., 2017) as companion of ROXs 12 A, based on its radial velocity and proper motion. We prove the equidistance of both stars with their Gaia DR2 astrometry, which also confirms their common proper motion.
[p]This companion was reported by (Hartman et al., 2020), who used the Gaia DR2 astrometry to confirm its companionship with the exoplanet host star HATS-48 A, as done in this work.
[q]NGTS-7 B was revealed by (Jackman et al., 2019) as companion of the exoplanet host star NGTS-7 A using Gaia DR2 astrometry, as done in this study.

models. Therefore, the properties of the companion were estimated via extrapolation from the two brightest sources of the used model isochrone.
- WD: The detected companion is a white dwarf.
- BD: The detected companion is a brown dwarf.

Finally, in **Table 5** we summarize all those detected companions, whose differential proper motion $\mu_{\mathrm{rel}}$ significantly exceeds their expected escape velocity $\mu_{\mathrm{rel}}$. Companions, which are already known to be members of hierarchical triple star systems, are indicated with the flag *** in the last column of this table.

Among all 289 targets, whose multiplicity was investigated in the study, whose results are presented in this paper, 41 binary and five hierarchical triple star systems with exoplanets were identified. This yields a multiplicity rate of the targets of 16 ± 2%, very well consistent with the multiplicity rate of exoplanet host stars of 15 ± 1%, reported before by Mugrauer (2019). This is as expected, as the sensitivities of the two surveys should agree well with each other, as the brightness and mass of their targets match, and the distance of the targets from this survey is on average about 40% smaller than that of the targets from Mugrauer (2019), resulting in a reduction in the distance modulus of only about 1 mag. In total, 61 companions (48 stars and 13 brown dwarfs) could be detected in the Gaia DR2 around the targets. The detected substellar companions are all listed as exoplanets in the EPE. The cumulative distribution functions of the derived properties (projected separation, mass and effective temperature) of theses companions, are illustrated in **Figures 3–5**. The separation-mass diagram of the companions is shown in **Figure 6**. As described above, the accurate Gaia DR2 astrometry proves the equidistance and common proper motion of all detected companions with the associated exoplanet hosts, and for the majority of these companions their differential proper motion to the exoplanet hosts is slower than their estimated escape velocity, facts that are expected for gravitationally bound systems. In contrast, the differential proper motion of the companions, which are listed in **Table 5**, exceeds their estimated escape velocity, possibly indicating a higher degree of multiplicity[4]. Indeed, one of these companions (51 Eri BC) is already known to be a close binary itself. The remaining two companions and their primaries are promising targets for follow-up observations to check their multiplicity status e.g. with high contrast AO imaging observations.

All detected companions exhibit projected separations to the associated exoplanet hosts in the range between 52 and 9,555 au (average separation of about 2,310 au). The highest companion frequency is found at projected separations between about 240 and 400 au and half of all companions are located at projected separations below about 1,240 au. The closest detected companion is K2-288 A, which is separated from the exoplanet host star K2-288 B by 52 au, and it is the only companion identified in this study within a projected separation of 100 au. The masses of the companions range between 0.016 and 1.66 $M_\odot$ (average mass of 0.36 $M_\odot$) and companions are found most frequently in the substellar mass

[4]Additional close companions either of the exoplanet hosts or of the companions force these objects on close orbits with high orbital velocities around a common barycenter that could induce the observed high differential velocities.

**TABLE 4** | The equatorial coordinates and derived physical properties of all detected companions.

| Companion | α (°) | δ (°) | $M_G$ (mag) | sep (au) | mass ($M_\odot$) | $T_{eff}$ (K) | Flags |
|---|---|---|---|---|---|---|---|
| HD 1160 C | 3.98858470355 | 4.25245524714 | $9.72^{+0.10}_{-0.13}$ | 648 | $0.378^{+0.021}_{-0.016}$ | $3503^{+25}_{-19}$ | BPRP PRI |
| Gliese 49 B | 15.83942593995 | 62.36588062663 | $11.35^{+0.41}_{-0.22}$ | 2,902 | $0.169^{+0.020}_{-0.030}$ | $3211^{+40}_{-74}$ | 2MA BPRP PRI |
| HD 8326 B | 20.54104760211 | −26.90734439784 | $11.48^{+0.04}_{-0.25}$ | 1747 | $0.198^{+0.023}_{-0.003}$ | $3257^{+37}_{-7}$ | 2MA BPRP PRI |
| HD 13167 B | 32.06020575541 | −24.69051459458 | $11.33^{+0.07}_{-0.06}$ | 3,001 | $0.211^{+0.006}_{-0.007}$ | $3279^{+9}_{-10}$ | 2MA BPRP |
| HR 858 B | 42.98571355919 | −30.81182706733 | $13.39^{+0.09}_{-0.11}$ | 267 | $0.112^{+0.003}_{-0.002}$ | $2926^{+20}_{-19}$ | BPRP PRI |
| HD 18015 B | 43.36225373946 | − 8.84661863284 | $6.62^{+0.04}_{-0.04}$ | 881 | $0.747^{+0.004}_{-0.004}$ | $4650^{+20}_{-18}$ | 2MA BPRP PRI |
| K2-288 A | 55.44420842474 | 18.26869720107 | $8.65^{+0.09}_{-0.09}$ | 52 | $0.534^{+0.010}_{-0.010}$ | $3777^{+30}_{-28}$ | 2MA |
| HD 23472 B | 55.46315889099 | −62.76539647729 | $12.79^{+0.07}_{-0.18}$ | 374 | $0.129^{+0.006}_{-0.002}$ | $3038^{+30}_{-13}$ | 2MA BPRP PRI |
| HD 24085 A | 56.19506729271 | −70.02706843481 | $2.90^{+0.39}_{-0.59}$ | 4,174 | $1.254^{+0.088}_{-0.058}$ | $6339^{+211}_{-139}$ | 2MA BPRP PRI EXT |
| HII 1348 C | 56.81444339267 | 24.39176993016 | $10.07^{+0.33}_{-0.31}$ | 5,155 | $0.322^{+0.048}_{-0.046}$ | $3436^{+58}_{-60}$ | 2MA BPRP PRI *** |
| HII 1348 D | 56.82474725542 | 24.37529892928 | $14.35^{+0.46}_{-0.37}$ | 7,872 | $0.055^{+0.005}_{-0.006}$ | $2602^{+78}_{-96}$ | BD 2MA BPRP *** |
| HATS-57 B | 60.94413061754 | −19.05596683949 | $10.25^{+0.05}_{-0.18}$ | 4,068 | $0.331^{+0.023}_{-0.007}$ | $3448^{+24}_{-7}$ | 2MA BPRP |
| FU Tau B | 65.89894960541 | 25.04979704793 | $12.62^{+0.49}_{-0.26}$ | 749 | $0.018^{+0.002}_{-0.003}$ | $2553^{+38}_{-71}$ | BD 2MA BPRP |
| DH Tau C | 67.42700661202 | 26.54688636442 | $3.64^{+0.17}_{-0.37}$ | 2071 | $1.655^{+0.228}_{-0.106}$ | $4837^{+164}_{-77}$ | 2MA BPRP PRI EXT |
| 51 Eri B (SB) | 69.40630139702 | − 2.49157819607 | $7.18^{+0.11}_{-0.27}$ | 1994 | $0.733^{+0.056}_{-0.024}$ | $3962^{+116}_{-49}$ | 2MA BPRP PRI *** |
| 2M 0441+23 AB[a] | 70.44024465438 | 23.03268965375 | $7.37^{+0.43}_{-0.96}$ | 1,483 | $0.241^{+0.147}_{-0.061}$ | $3308^{+300}_{-138}$ | 2MA BPRP |
| NGTS-6 B | 75.79692465277 | −30.40013000839 | $9.23^{+0.14}_{-0.10}$ | 1,667 | $0.457^{+0.013}_{-0.018}$ | $3618^{+21}_{-29}$ | 2MA BPRP PRI |
| AB Dor BD | 82.18603484814 | −65.44557858318 | $9.08^{+0.44}_{-0.52}$ | 136 | $0.466^{+0.061}_{-0.059}$ | $3645^{+167}_{-104}$ | 2MA BPRP PRI *** |
| HD 39855 B | 88.62713212305 | −19.70163948841 | $8.02^{+0.13}_{-0.23}$ | 250 | $0.598^{+0.024}_{-0.014}$ | $3978^{+103}_{-41}$ | 2MA BPRP PRI |
| NGTS-10 B | 91.87213254706 | −25.59461438962 | $7.27^{+0.61}_{-1.21}$ | 364 | $0.665^{+0.121}_{-0.059}$ | $4327^{+606}_{-284}$ | |
| L2 Pup B | 108.39678197580 | −44.63427669967 | $11.39^{+0.17}_{-0.33}$ | 2,101 | $0.203^{+0.032}_{-0.012}$ | $3270^{+49}_{-26}$ | |
| HIP 38594 B | 118.48449010900 | −25.39952189079 | $14.43^{+0.26}_{-0.78}$ | 7,116 | ~ 0.6 | | WD 2MA BPRP PRI |
| WASP-180 B | 123.39313443835 | − 1.98380547425 | $4.64^{+0.06}_{-0.16}$ | 1,244 | $1.057^{+0.029}_{-0.011}$ | $5778^{+93}_{-36}$ | 2MA BPRP PRI |
| HD 79211 A | 138.58391575741 | 52.68415915741 | $7.59^{+0.21}_{-0.33}$ | 108 | $0.644^{+0.034}_{-0.022}$ | $4180^{+153}_{-97}$ | 2MA BPRP PRI |
| HD 85628 B | 147.57796550484 | −66.11477795490 | $7.38^{+0.23}_{-0.15}$ | 744 | $0.675^{+0.016}_{-0.025}$ | $4282^{+66}_{-104}$ | BPRP PRI |
| TOI 717 B | 147.98872815946 | 2.11708155887 | $9.72^{+0.02}_{-0.13}$ | 2,275 | $0.398^{+0.017}_{-0.003}$ | $3519^{+25}_{-3}$ | 2MA BPRP PRI |
| G 196-3 B | 151.08506490419 | 50.38228242112 | $17.41^{+0.48}_{-0.49}$ | 350 | $0.032^{+0.002}_{-0.002}$ | $1987^{+94}_{-93}$ | BD 2MA BPRP |
| LTT 3780 B | 154.64934761666 | −11.71834621199 | $12.27^{+0.34}_{-0.26}$ | 347 | $0.149^{+0.014}_{-0.014}$ | $3127^{+43}_{-58}$ | 2MA BPR PPRI |
| MASCARA-3 B | 161.90924448675 | 71.65515762432 | $7.83^{+0.12}_{-0.28}$ | 200 | $0.625^{+0.030}_{-0.013}$ | $4074^{+126}_{-53}$ | |
| 2M J1101-7732 B | 165.33045751133 | −77.54374799758 | $12.48^{+0.14}_{-0.14}$ | 264 | $0.019^{+0.001}_{-0.001}$ | $2574^{+21}_{-21}$ | BD |
| WASP-175 B | 166.31900970217 | −34.12073886500 | $5.46^{+0.10}_{-0.11}$ | 3,971 | $0.919^{+0.018}_{-0.016}$ | $5290^{+65}_{-60}$ | 2MA BPR PPRI |
| CHXR 73 C | 166.56385863699 | −77.63060598303 | $8.04^{+1.03}_{-1.03}$ | 8,808 | $0.235^{+0.148}_{-0.112}$ | $3280^{+295}_{-260}$ | 2MA BPRP |
| GJ 414 B | 167.76359381364 | 30.44392150823 | $8.06^{+0.32}_{-0.57}$ | 406 | $0.587^{+0.056}_{-0.034}$ | $3971^{+249}_{-110}$ | 2MABPRP PRI |
| HD 97334 BC[b] | 168.10555672848 | 35.80289455668 | $18.16^{+0.04}_{-0.19}$ | 2036 | $0.028^{+0.001}_{-0.001}$ | $1845^{+36}_{-8}$ | BD 2MA BPRP |
| HD 233832 B | 171.51750545565 | 50.37622350226 | $8.64^{+0.11}_{-0.21}$ | 290 | $0.531^{+0.022}_{-0.012}$ | $3775^{+68}_{-36}$ | 2MA BPRP PRI |
| 2M J1155-7919 B | 178.76276748600 | −79.32082818366 | $14.48^{+0.02}_{-0.06}$ | 582 | $0.016^{+0.001}_{-0.001}$ | $2366^{+10}_{-2}$ | BD 2MA BPRP |
| NGTS-5 B | 221.06499706987 | 5.60206193982 | $9.67^{+0.12}_{-0.11}$ | 8,323 | $0.405^{+0.014}_{-0.016}$ | $3530^{+22}_{-20}$ | 2MA BPRP |
| 2M J1450-7841 B | 222.67064914833 | −78.69407266366 | $15.35^{+0.51}_{-0.51}$ | 387 | $0.031^{+0.005}_{-0.003}$ | $2328^{+114}_{-100}$ | BD 2MA BPRP |
| WASP-189 B | 225.68920534342 | − 3.03062676806 | $9.12^{+0.23}_{-0.16}$ | 942 | $0.479^{+0.021}_{-0.030}$ | $3646^{+33}_{-48}$ | 2MA BPRP PRI |
| HIP 73990 D | 226.82470360183 | −29.49738818566 | $8.33^{+0.45}_{-0.64}$ | 5,234 | $0.470^{+0.151}_{-0.098}$ | $3576^{+191}_{-107}$ | 2MA BPRP PRI |
| TOI 905 B | 227.66059753260 | −71.36174373792 | $10.93^{+0.17}_{-0.14}$ | 358 | $0.251^{+0.014}_{-0.016}$ | $3340^{+21}_{-25}$ | |
| 2M 1510 B | 227.69777941730 | −28.30671294175 | $15.13^{+0.03}_{-0.14}$ | 249 | $0.033^{+0.001}_{-0.001}$ | $2376^{+31}_{-6}$ | BD 2MA BPRP |
| β Cir B | 229.33920903332 | −58.85886078926 | $16.91^{+0.16}_{-0.23}$ | 6,187 | $0.063^{+0.002}_{-0.002}$ | $2159^{+47}_{-48}$ | BD 2MA BPRP |
| KELT-23 B | 232.14912993468 | 66.35793842725 | $9.94^{+0.05}_{-0.10}$ | 575 | $0.368^{+0.014}_{-0.007}$ | $3487^{+15}_{-7}$ | 2MA BPRP PRI |
| K2-290 C | 234.85788601749 | −20.20202286624 | $10.51^{+0.27}_{-0.26}$ | 3,094 | $0.292^{+0.033}_{-0.026}$ | $3404^{+38}_{-41}$ | 2MA BPRP*** |
| GQ Lup C | 237.30537201266 | −35.65336961027 | $9.70^{+0.42}_{-0.34}$ | 2,446 | $0.075^{+0.016}_{-0.015}$ | $2897^{+14}_{-33}$ | 2MA BPRP |
| HIP 77900 B | 238.62692763313 | −27.33270712891 | $13.48^{+0.05}_{-0.16}$ | 3,374 | $0.020^{+0.001}_{-0.001}$ | $2519^{+22}_{-8}$ | BD BPRP |
| USco 1602-2401 B[c] | 240.71312906858 | −24.03074240242 | $8.69^{+0.12}_{-0.12}$ | 1,038 | $0.238^{+0.016}_{-0.017}$ | $3280^{+25}_{-27}$ | 2MA BPRP PRI |
| HIP 79098 C | 242.20150369275 | −23.68925441843 | $9.82^{+0.24}_{-0.15}$ | 9,555 | $0.159^{+0.013}_{-0.020}$ | $3176^{+24}_{-40}$ | 2MA BPRP PRI *** |
| USco 1610-1913 B | 242.63466253957 | −19.21910506083 | $12.71^{+0.39}_{-0.39}$ | 777 | $0.025^{+0.003}_{-0.003}$ | $2615^{+47}_{-47}$ | BD 2MA BPRP |
| USco 1612-1800 B | 243.20402838620 | −18.01380384763 | $12.50^{+0.39}_{-0.39}$ | 504 | $0.026^{+0.003}_{-0.003}$ | $2642^{+48}_{-48}$ | BD BPRP |
| ROXs 12 C | 246.61560598363 | −25.45695531769 | $7.28^{+1.00}_{-1.00}$ | 5,095 | $0.474^{+0.259}_{-0.181}$ | $3657^{+343}_{-289}$ | 2MA BPR PPRI |
| HATS-48 B | 288.66902407326 | −59.57941400923 | $11.71^{+0.37}_{-0.19}$ | 1,444 | $0.181^{+0.013}_{-0.022}$ | $3219^{+30}_{-60}$ | 2MA BPRP |
| GJ 752 B | 289.23745710752 | 5.14456304678 | $14.04^{+0.17}_{-0.28}$ | 446 | $0.098^{+0.005}_{-0.002}$ | $2785^{+60}_{-36}$ | 2MA BPRP PRI |
| HD 181234 B | 290.00108472870 | −9.32417966740 | $10.46^{+0.07}_{-0.20}$ | 247 | $0.297^{+0.026}_{-0.007}$ | $3412^{+29}_{-11}$ | 2MA BPRP PRI |
| Wendelstein-1 B | 299.04791069915 | 17.56797448132 | $11.43^{+0.43}_{-0.47}$ | 3,632 | $0.202^{+0.047}_{-0.030}$ | $3264^{+72}_{-70}$ | 2MA BPRP |
| 2M J2126-81 B | 321.71158783493 | −81.67526360458 | $17.84^{+0.05}_{-0.43}$ | 7,427 | $0.020^{+0.001}_{-0.004}$ | $1851^{+41}_{-77}$ | BD 2MA BPRP |
| TOI 132 B | 338.40325545731 | −43.44166603901 | $12.21^{+0.14}_{-0.16}$ | 3,231 | $0.152^{+0.009}_{-0.006}$ | $3137^{+27}_{-24}$ | 2MA BPRP |
| NGTS-7 B | 352.52202473338 | −38.97006605140 | $9.32^{+0.50}_{-0.50}$ | 156 | $0.384^{+0.097}_{-0.091}$ | $3495^{+102}_{-97}$ | |
| DS Tuc B | 354.91457052896 | −69.19458723114 | $5.86^{+0.10}_{-0.24}$ | 237 | $0.834^{+0.060}_{-0.027}$ | $5040^{+180}_{-79}$ | 2MA BPRP PRI |
| 1RXS J2351+3127 C | 357.93142859121 | 31.45083817280 | $9.61^{+0.04}_{-0.43}$ | 5,427 | $0.394^{+0.057}_{-0.007}$ | $3522^{+98}_{-8}$ | 2MA BPRP PRI |

[a]*2M 0441+23 B is a close brown dwarf companion of 2M 0441+23 A.*
[b]*HD 97334 BC is a binary brown dwarf system.*

[c]The brown dwarf USco 1602-2401 B was detected by Aller et al. (2013) and its possible companionship to USco 1602-2401 A, was revealed with photometry and follow-up spectroscopy, which was finally proven in this study with the Gaia DR2 astrometry of the companion, i.e. confirmation of equidistance, and common proper motion, as well as test for gravitational stability. USco 1602-2401 B is one of 14 reported substellar companions, detected by Gaia, which were also characterized in this study using their Gaia DR2 astro- and photometry. In general, the derived mass of these substellar companions agrees well with the mass given in the literature, with a deviation of only a few $M_{Jup}$, on average. In contrast, for USco 1602-2401 B Aller et al. (2013) derived a mass of $41^{+20}_{-13}M_{Jup}$ at an age of 5 Myr ($47^{+20}_{-18}M_{Jup}$ at 10 Myr) adopting a distance of about 145 pc and no extinction. With the Gaia DR2 parallax and the Starhorse extinction estimate of the primary star and the G-band photometry of the companion we obtained a significantly higher mass of $0.238^{+0.016}_{-0.017}M_\odot$ at 5 Myr ($0.309^{+0.020}_{-0.019}M_\odot$ at 10 Myr). Adopting $A_G$ = 0 mag yields a mass of the companion of $0.071^{+0.001}_{-0.001}M_\odot$ for 5 Myr, and $0.104^{+0.001}_{-0.001}M_\odot$ for 10 Myr, respectively. Therefore, we classify this companion here as low-mass star.

**TABLE 5 |** List of all detected companions, whose differential proper motion $\mu_{rel}$ exceeds their estimated escape velocity $\mu_{esc}$.

| Companion | $\mu_{rel}$ (mas/yr) | $\mu_{esc}$ (mas/yr) | |
|---|---|---|---|
| 51 Eri B (SB) | 19.04 ± 0.71 | 11.298 ± 0.144 | *** |
| HIP 38594 B | 6.44 ± 0.24 | 4.965 ± 0.082 | |
| TOI 905 B | 7.67 ± 0.76 | 3.090 ± 0.144 | |

regime between 0.016 up to 0.033 $M_\odot$, while more massive companions are detected at a lower but constant frequency up to about 0.7 $M_\odot$, and only about 10% of all the detected companions exhibit masses larger than 0.7 $M_\odot$. The companions exhibit effective temperatures in the range between about 1850 and 6350 K (average temperature of about 3400 K), which corresponds to spectral types of L3 to F6 (M3, on average), according to the $T_{\rm eff} - SpT$ relation[5] from (Pecaut and Mamajek, 2013).

In general the effective temperature of the detected companions, determined with their derived absolute G-band magnitude, using the evolutionary Baraffe et al. (2015) models, agree well with their Gaia DR2 Apsis-Priam temperature estimate (if available) with a characteristic deviation of about ±350 K, consistent with the typical uncertainty of the different temperature estimates, which is in the order of about 330 K. Only in the case of HIP 38594 B the temperature estimate, based on the absolute G-band photometry of the companion significantly deviates by more than 2300 K from its Apsis-Priam temperature estimate, which is also about 900 K higher than the one of the associated exoplanet host star HIP 38594 A. Furthermore, the companion appears bluer ($\Delta(G_{BP} - G_{RP}) = -0.669 \pm 0.004$ mag) than its primary although it is about 7 mag fainter in the G-band than the exoplanet host star. The intrinsic faintness and high temperature of HIP 38594 B clearly indicates that this companion is a white dwarf. This conclusion is consistent with the results of Subasavage et al. (2008), who have already classified the companion spectroscopically as a white dwarf, and have denote it as WD 0751-252. For this degenerated companion we adopt here a mass of about 0.6 $M_\odot$.

In **Figure 7** the G-band magnitude difference of all detected companions to the associated exoplanet hosts is plotted vs. their angular separation. For comparison we show as dashed line in this figure the estimate of the Gaia detection limit, reported by Mugrauer (2019) which was further constrained by Mugrauer and Michel (2020). Companions of exoplanet hosts brighter than 12.8 mag are plotted as open circles those of hosts, which are fainter than that magnitude limit, as filled black circles, respectively. A magnitude difference of about 5 mag is reached at an angular separation of about two arcsec, consistent with the estimate of the Gaia detection limit, determined by Mugrauer (2019). Only two companions significantly exceed the limit estimate, namely K2-288 A at an angular separation of about 0.8 arcsec with $\Delta G \sim 1.2$ mag and HIP 77900 B, at 22.3 arcsec with $\Delta G \sim 13.5$ mag. While K2-288 A is a companion of a target fainter than $G = 12.8$ mag for which Gaia reaches a higher sensitivity at angular separations slightly below one arcsec (up to 3 mag, as described by Mugrauer and Michel, 2020) the detection of HIP 77900 B indicates that the given limit estimate might be too conservative at angular separations beyond about 20 arcsec.

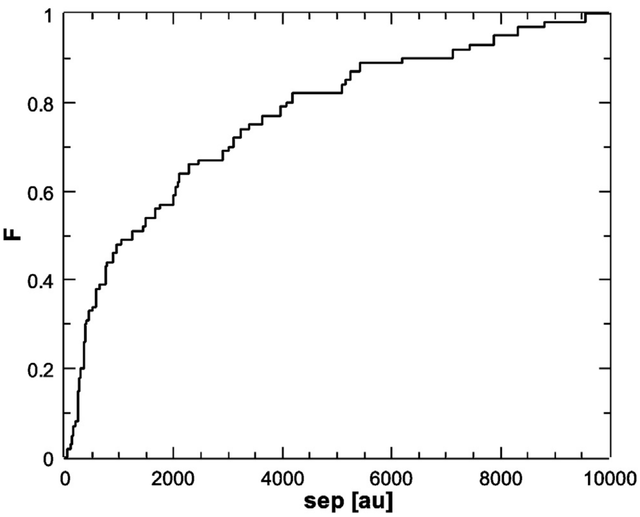


**FIGURE 3 |** The cumulative distribution function of the projected separation (sep) of all detected companions to the associated exoplanet hosts.

## 4 SUMMARY AND OUTLOOK

The study, presented here, is a continuation of a survey, which was initiated at the Astrophysical Institute and University Observatory Jena, to investigate the multiplicity status of exoplanet hosts and to characterize the properties of their detected (sub)stellar companions, using accurate Gaia astro-

[5]Online available at: http://www.pas.rochester.edu/~emamajek/EEM_dwarf_UBVIJHK_colors_Teff.txt

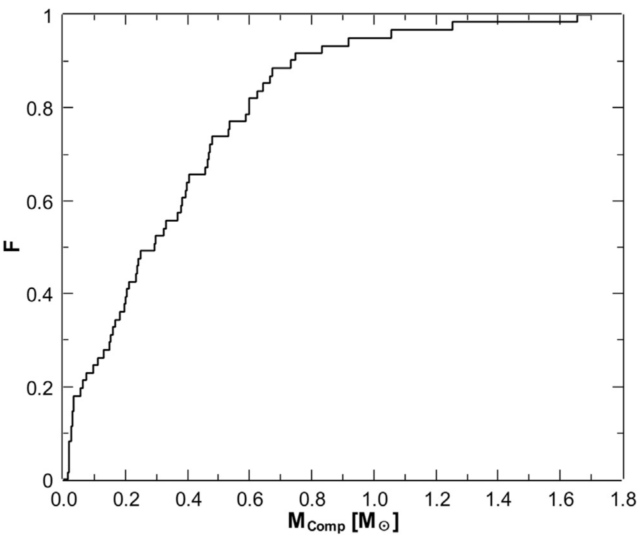


**FIGURE 4 |** The cumulative distribution function of the mass of all companions, detected in this study.

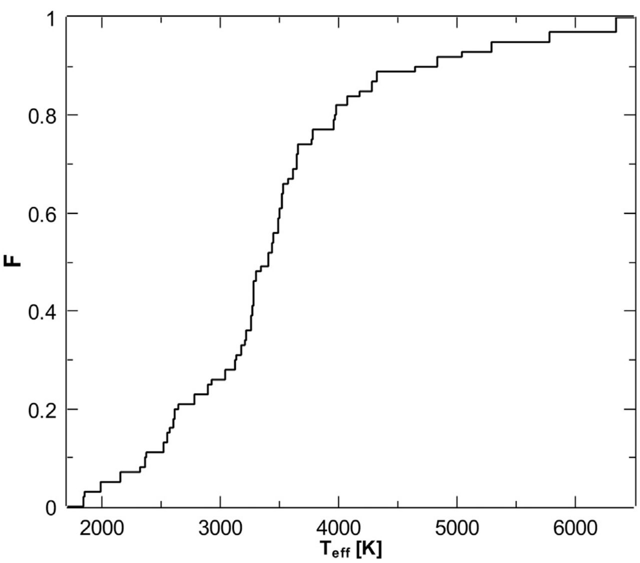


**FIGURE 5 |** The cumulative distribution function of the effective temperature of all detected companions.

and photometry. In this paper the multiplicity of 289 exoplanet hosts was explored and (sub)stellar companions were detected around 60 targets. The companionship of these objects with the exoplanet hosts could be proven with their accurate Gaia DR2 astrometry (equidistance, common proper motion, and differential proper motion smaller than the expected escape velocity). The mass and effective temperature of all companions were determined with their derived absolute G-band photometry and the Baraffe et al. (2015) evolutionary models of (sub)stellar objects. In total, 61 companions (beside 48

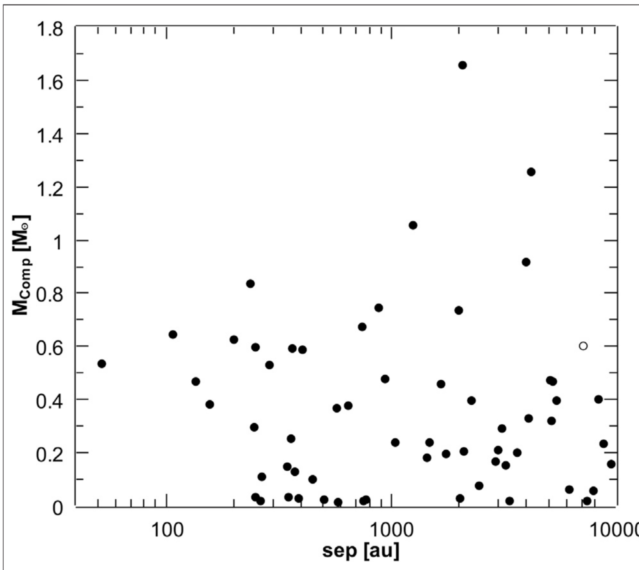


**FIGURE 6 |** The mass of all companions, detected in this study, plotted over their projected separation (sep) to the associated exoplanet hosts. The white dwarf companion HIP 38594 B, is illustrated as open circle.

stellar companions, among them the white dwarf HIP 38594 B, also 13 brown dwarfs) were detected in this project, and 14 of these objects are neither listed in the WDS as companion (-candidate)s of the targets nor were described in the literature before. A total of 41 binary and five triple star systems with exoplanets, were identified in this study, yielding a multiplicity rate of the targets of about 16%, which is very well consistent with the multiplicity rate of exoplanet host stars, reported by Mugrauer (2019). Following the standard procedure of our survey, all detected companions and their derived properties will be made available online in the VizieR database. The survey, whose latest results are presented here, is an ongoing project as more and more exoplanet hosts are detected by different planet detection methods, whose multiplicity status needs to be investigated. Furthermore, there are sources, listed in the Gaia DR2, within the applied search radius around the targets, which still lack a five parameter astrometric solution. Hence, further companions of the exoplanet hosts, investigated here, should exist, whose companionship can be proven with accurate astrometric measurements, provided by future data releases of the ESA-Gaia mission, e.g. the Gaia EDR3, planed to be published end of 2020.

The results of this survey, which is mainly sensitive for wide companions of exoplanet hosts, combined with those of our currently ongoing large high contrast imaging surveys (sensitive for close companions), carried out with SPHERE/VLT and AstraLux/CAHA (first results are already published e.g. by Ginski et al., 2020) will yield a complete characterization of the multiplicity status of the observed targets. This will eventually allow to draw conclutions on the impact of the stellar multiplicity on the formation process of planets and the evolution of their orbits.

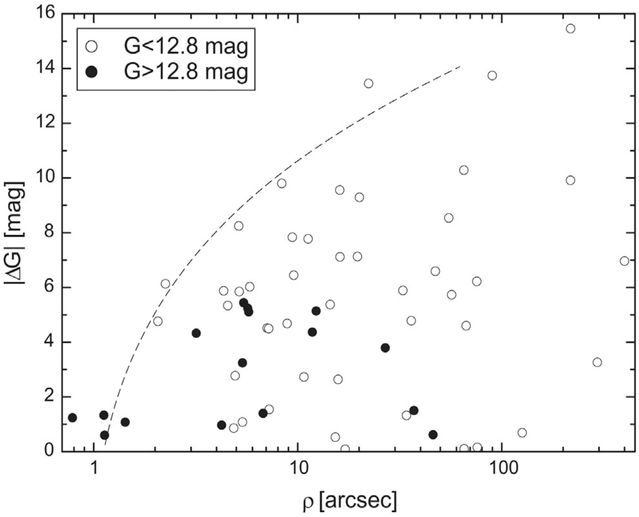


**FIGURE 7 |** The G-band magnitude difference of all detected companions, plotted over their angular separation to the associated exoplanet hosts.

## DATA AVAILABILITY STATEMENT

Publicly available datasets were analyzed in this study. This data can be found here: https://vizier.u-strasbg.fr/viz-bin/VizieR-3?-source=I/345/gaia2&-out.max=50&-out.form=HTML%20Table&-out.add=_r&-out.add=_RAJ,_DEJ&-sort=_r&-oc.form=sexa.

## AUTHOR CONTRIBUTIONS

K-UM and MM have worked together on the data analysis and its publication.


## ACKNOWLEDGMENTS

We thank the two anonymous referees for their helpful and constructive comments on the manuscript. We made use of data from: (1) the Simbad and VizieR databases, both operated at CDS in Strasbourg, France. (2) the European Space Agency (ESA) mission Gaia (https://www.cosmos.esa.int/gaia), processed by the Gaia Data Processing and Analysis Consortium (DPAC, https://www.cosmos.esa.int/web/gaia/dpac/consortium). Funding for the DPAC has been provided by national institutions, in particular the institutions participating in the Gaia Multilateral Agreement. (3) the Two Micron All Sky Survey, which is a joint project of the University of Massachusetts and the Infrared Processing and Analysis Center/California Institute of Technology, funded by the National Aeronautics and Space Administration and the National Science Foundation.


## REFERENCES


Aller, K. M., Kraus, A. L., Liu, M. C., Burgett, W. S., Chambers, K. C., Hodapp, K. W., et al. (2013). A pan-STARRS + UKIDSS search for young, wide planetary-mass companions in upper scorpius. *ApJ* 773, 63. doi:10.1088/0004-637X/773/1/63

Anders, F., Khalatyan, A., Chiappini, C., Queiroz, A. B., Santiago, B. X., Jordi, C., et al. (2019). Photo-astrometric distances, extinctions, and astrophysical parameters for Gaia DR2 stars brighter than G = 18. *A&A* 628, A94. doi:10.1051/0004-6361/201935765

Bailer-Jones, C. A. L., Andrae, R., Arcay, B., Astraatmadja, T., Bellas-Velidis, I., Berihuete, A., et al. (2013). TheGaiaastrophysical parameters inference system (Apsis). *A&A* 559, A74. doi:10.1051/0004-6361/201322344

Baraffe, I., Homeier, D., Allard, F., and Chabrier, G. (2015). New evolutionary models for pre-main sequence and main sequence low-mass stars down to the hydrogen-burning limit. *A&A* 577, A42. doi:10.1051/0004-6361/201425481

Basri, G. (2000). Observations of Brown dwarfs. *Annu. Rev. Astron. Astrophys.* 38, 485–519. doi:10.1146/annurev.astro.38.1.485

Bowler, B. P., and Hillenbrand, L. A. (2015). Near-infrared spectroscopy of 2M0441+2301 AabBab: a quadruple system spanning the stellar to planetary mass regimes. *ApJ* 811, L30. doi:10.1088/2041-8205/811/2/L30

Bowler, B. P., Kraus, A. L., Bryan, M. L., Knutson, H. A., Brogi, M., Rizzuto, A. C., et al. (2017). The young substellar companion ROXs 12 B: near-infrared spectrum, system Architecture, and spin-orbit misalignment. *AJ* 154, 165. doi:10.3847/1538-3881/aa88bd

Bowler, B. P., Liu, M. C., Shkolnik, E. L., Dupuy, T. J., Cieza, L. A., Kraus, A. L., et al. (2012). Planets around low-mass stars (PALMS). I. A substellar companion to the young M dwarf 1RXS J235133.3+312720. *ApJ* 753, 142. doi:10.1088/0004-637X/753/2/142

Burgasser, A. J., Looper, D. L., and Kirkpatrick, J. D. (2017). A candidate wide Brown dwarf binary in the argus association: 2MASS J14504216-7841413 and 2MASS J14504113-7841383. *Res. Notes AAS* 1, 42. doi:10.3847/2515-5172/aa9ff0

Dickson-Vandervelde, D. A., Wilson, E. C., and Kastner, J. H. (2020). Identification of the youngest known substellar object within ~100 pc. *Res. Notes AAS* 4, 25. doi:10.3847/2515-5172/ab7344

Dorval, P., Talens, G. J. J., Otten, G. P. P. L., Brahm, R., Jordán, A., Torres, P., et al. (2020). MASCARA-4 b/bRing-1 b: A retrograde hot Jupiter around a bright A-type star. *A&A* 635, A60. doi:10.1051/0004-6361/201935611

Duchêne, G., and Kraus, A. (2013). Stellar multiplicity. *Annu. Rev. Astron. Astrophys.* 51, 269–310. doi:10.1146/annurev-astro-081710-102602

Feinstein, A. D., Schlieder, J. E., Livingston, J. H., Ciardi, D. R., Howard, A. W., Arnold, L., et al. (2019). K2-288Bb: a small temperate planet in a low-mass binary system discovered by citizen scientists. *AJ* 157, 40. doi:10.3847/1538-3881/aafa70

Gaia CollaborationBrown, A. G. A., Vallenari, A., Prusti, T., de Bruijne, J. H. J., Babusiaux, C., et al. (2018). Gaia Data Release 2. Summary of the contents and survey properties. *A&A* 616, A1. doi:10.1051/0004-6361/201833051

Geißler, K., Metchev, S. A., Pham, A., Larkin, J. E., McElwain, M., and Hillenbrand, L. A. (2012). A substellar common proper-motion companion to the pleiad H II 1348. *ApJ* 746, 44. doi:10.1088/0004-637X/746/1/44

Ginski, C., Mugrauer, M., Adam, C., Vogt, N., and van Holstein, R. (2020). How many suns are in the sky? A sphere multiplicity survey of exoplanet host stars I – Four new close stellar companions including a white dwarf. Available at: http://arxiv.org/abs/2009.10363.

Hartman, J. D., Jordán, A., Bayliss, D., Bakos, G. Á., Bento, J., Bhatti, W., et al. (2020). HATS-47b, HATS-48Ab, HATS-49b, and HATS-72b: four warm giant planets transiting K dwarfs. *AJ* 159, 173. doi:10.3847/1538-3881/ab7821

Hinkley, S., Kraus, A. L., Ireland, M. J., Cheetham, A., Carpenter, J. M., Tuthill, P., et al. (2015). Discovery of seven companions to intermediate-mass stars with extreme mass ratios in the scorpius-centaurus association. *ApJ* 806, L9. doi:10.1088/2041-8205/806/1/L9

Hjorth, M., Justesen, A. B., Hirano, T., Albrecht, S., Gandolfi, D., Dai, F., et al. (2019). K2-290: a warm Jupiter and a mini-Neptune in a triple-star system. *MNRAS* 484, 3522–3536. doi:10.1093/mnras/stz139

Itoh, Y., Hayashi, M., Tamura, M., Tsuji, T., Oasa, Y., Fukagawa, M., et al. (2005). A young Brown dwarf companion to DH tauri. *ApJ* 620, 984–993. doi:10.1086/427086

Jackman, J. A. G., Wheatley, P. J., Bayliss, D., Gill, S., Hodgkin, S. T., Burleigh, M. R., et al. (2019). NGTS-7Ab: an ultrashort-period brown dwarf transiting a tidally locked and active M dwarf. *MNRAS* 489, 5146–5164. doi:10.1093/mnras/stz2496

Janson, M., Asensio-Torres, R., André, D., Bonnefoy, M., Delorme, P., Reffert, S., et al. (2019). The B-Star Exoplanet Abundance Study: a co-moving 16-25 MJup companion to the young binary system HIP 79098. *A&A* 626, A99. doi:10.1051/0004-6361/201935687

Johns, D., Reed, P. A., Rodriguez, J. E., Pepper, J., Stassun, K. G., Penev, K., et al. (2019). KELT-23Ab: a hot Jupiter transiting a near-solar twin close to the TESS and JWST continuous viewing zones. *AJ* 158, 78. doi:10.3847/1538-3881/ab24c7

Kraus, A. L., Ireland, M. J., Cieza, L. A., Hinkley, S., Dupuy, T. J., Bowler, B. P., et al. (2014). Three wide planetary-mass companions to FW Tau, ROXs 12, and ROXs 42B. *ApJ* 781, 20. doi:10.1088/0004-637X/781/1/20

Mason, B. D., Wycoff, G. L., Hartkopf, W. I., Douglass, G. G., and Worley, C. E. (2001). The 2001 US naval observatory Double star CD-ROM. I. The Washington Double star catalog. *AJ* 122, 3466. doi:10.1086/323920

McCormac, J., Gillen, E., Jackman, J. A. G., Brown, D. J. A., Bayliss, D., Wheatley, P. J., et al. (2020). NGTS-10b: the shortest period hot Jupiter yet discovered. *MNRAS* 493, 126–140. doi:10.1093/mnras/staa115

Mugrauer, M., and Ginski, C. (2015). High-contrast imaging search for stellar and substellar companions of exoplanet host stars. *MNRAS* 450, 3127–3136. doi:10.1093/mnras/stv771

Mugrauer, M., Ginski, C., and Seeliger, M. (2014). New wide stellar companions of exoplanet host stars. *MNRAS* 439, 1063–1070. doi:10.1093/mnras/stu044

Mugrauer, M., and Michel, K. U. (2020). Gaia search for stellar companions of TESS objects of interest. Available at: http://arxiv.org/abs/2009.12234.

Mugrauer, M. (2019). Search for stellar companions of exoplanet host stars by exploring the second ESA-Gaia data release. *MNRAS* 490, 5088–5102. doi:10.1093/mnras/stz2673

Neuhäuser, R., Guenther, E. W., Wuchterl, G., Mugrauer, M., Bedalov, A., and Hauschildt, P. H. (2005). Evidence for a co-moving sub-stellar companion of GQ Lup. *A&A* 435, L13–L16. doi:10.1051/0004-6361:200500104

Nielsen, E. L., Liu, M. C., Wahhaj, Z., Biller, B. A., Hayward, T. L., Boss, A., et al. (2012). The gemini NICI planet-finding campaign: discovery of a multiple system orbiting the young A star HD 1160. *ApJ* 750, 53. doi:10.1088/0004-637X/750/1/53

Nielsen, L. D., Bouchy, F., Turner, O. D., Anderson, D. R., Barkaoui, K., Benkhaldoun, Z., et al. (2019). WASP-169, WASP-171, WASP-175, and WASP-182: three hot Jupiters and one bloated sub-Saturn mass planet discovered by WASP-South. *MNRAS* 489, 2478–2487. doi:10.1093/mnras/stz2351

Ochsenbein, F., Bauer, P., and Marcout, J. (2000). The VizieR database of astronomical catalogues. *Astron. Astrophys. Suppl. Ser.* 143, 23–32. doi:10.1051/aas:2000169

Pecaut, M. J., and Mamajek, E. E. (2013). Intrinsic colors, temperatures, and bolometric corrections of pre-main-sequence stars. *ApJS* 208, 9. doi:10.1088/0067-0049/208/1/9

Ricker, G. R., Winn, J. N., Vanderspek, R., Latham, D. W., Bakos, G. Á., Bean, J. L., et al. (2015). Transiting exoplanet survey satellite (TESS). *JATIS* 1, 014003. doi:10.1117/1.JATIS.1.1.014003

Rodriguez, J. E., Eastman, J. D., Zhou, G., Quinn, S. N., Beatty, T. G., Penev, K., et al. (2019). KELT-24b: a 5M J planet on a 5.6 day well-aligned orbit around the young V = 8.3 F-star HD 93148. *AJ* 158, 197. doi:10.3847/1538-3881/ab4136

Schneider, J., Dedieu, C., Le Sidaner, P., Savalle, R., and Zolotukhin, I. (2011). Defining and cataloging exoplanets: the exoplanet.eu database. *A&A* 532, A79. doi:10.1051/0004-6361/201116713

Skrutskie, M. F., Cutri, R. M., Stiening, R., Weinberg, M. D., Schneider, S., Carpenter, J. M., et al. (2006). The two Micron all sky survey (2MASS). *Astron. J.* 131, 1163–1183. doi:10.1086/498708

Smart, R. L., and Nicastro, L. (2014). The initialGaiasource list. *A&A* 570, A87. doi:10.1051/0004-6361/201424241

Subasavage, J. P., Henry, T. J., Bergeron, P., Dufour, P., and Hambly, N. C. (2008). The solar neighborhood. Xx. Discovery and characterization of 21 new nearby white dwarf systems. *Astronomical J.* 136, 899–908. doi:10.1088/0004-6256/136/3/899

Triaud, A. H. M. J., Burgasser, A. J., Burdanov, A., Kunovac Hodžić, V., Alonso, R., Bardalez Gagliuffi, D., et al. (2020). An eclipsing substellar binary in a young triple system discovered by speculoos. *Nat. Astron.* 4, 650–657. doi:10.1038/s41550-020-1018-2

van Leeuwen, F. (2007). Validation of the new Hipparcos reduction. *A&A* 474, 653–664. doi:10.1051/0004-6361:20078357

Vanderburg, A., Huang, C. X., Rodriguez, J. E., Becker, J. C., Ricker, G. R., Vanderspek, R. K., et al. (2019). Tess spots a compact system of super-earths around the naked-eye star HR 858. *ApJ* 881, L19. doi:10.3847/2041-8213/ab322d


**Conflict of Interest:** The authors declare that the research was conducted in the absence of any commercial or financial relationships that could be construed as a potential conflict of interest.